Chapter 5

Synthesis and mesomorphic properties of

Part I

(i) **2-Cyano-1, 3-phenylene bis [4-(4-*n*-alkyloxycarbonylphenyliminomethyl)benzoates]**

(ii) **2-Nitro-1, 3-phenylene bis [4-(4-*n*-alkyloxycarbonylphenyliminomethyl)benzoates]**

Part II

(iii) **2-Cyano-1, 3-phenylene bis [4-(4-*n*-alkyloxycarbonylbenzylideneamino)benzoates]**

(iv) **2-Nitro-1, 3-phenylene bis [4-(4-*n*-alkyloxycarbonylbenzylideneamino)benzoates]**

Introduction

Amongst all the mesophases exhibited by bent-core (BC) compounds, the most beautiful and fascinating textures are shown by the B_7 phase. The B_7 phase was first observed [1] in 2-nitro-1, 3-phenylene bis [4-(4-*n*-alkyloxyphenyliminomethyl)benzoates] (W1044, *n*=8). Subsequently, this phase was observed [2-5] in a number of compounds derived from 2-cyanoresorcinol. Apart from these, B_7 phase was also reported in five-ring bent-core mesogens derived from 5-fluororesorcinol and containing a chloro substituent at the terminal rings [6]. The common feature of the B_7 phase exhibited by all these compounds is that, the X-ray diffraction (XRD) data is similar. The mesophase shows a medium angle reflection in addition to several small angle reflections and of course the diffuse wide-angle reflection. The mesophase is non-switchable even at a fairly high applied voltage and exhibit several beautiful textures. One such characteristic texture of the B_7 phase is the growth of helical or spiral filaments on slow cooling from the isotropic phase. In addition, it also exhibits banana-leaf shape domains, striped focal-conics, circular and oval domains, myelinic and checker-board-like textures.

There are a number of BC compounds varying in their chemical nature but without the polar cyano or nitro group in the angular position and belonging to different homologous series [7-11] which exhibit the helical filamentary texture, and in some cases other variants as well, which are assigned the symbol B_7. Typically, these are smectic phases which show either ferroelectric or antiferroelectric switching characteristics and more importantly the medium angle reflection in the XRD pattern is absent but satellites of weak intensity are seen behind the layer reflections. It has been recommended to assign the general symbol B_7' to these phases and a detailed analysis of the B_7 phases have been very nicely reviewed recently [12].

Coleman *et al*. [13] carried out an in-depth analysis of the mesophase exhibited by compound MHOBOW [9] using synchrotron X-ray, micro-beam X-ray, freeze fracture transmission electron microscopy (FFTEM) and depolarized transmission and reflection light microscopy. The mesophase has been assigned the symbol B_7, although it exhibits SmC_sP_F structure [9] and XRD pattern is different from that of the classical B_7 phase [1-6].

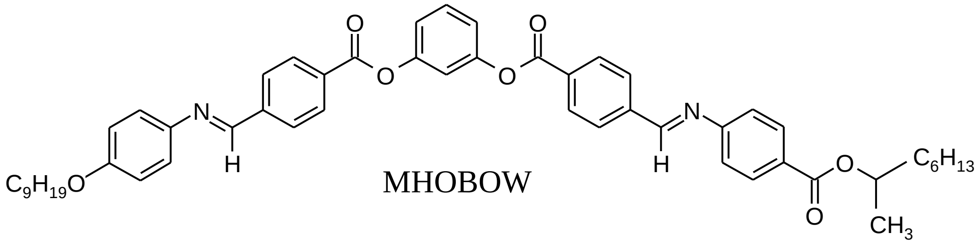

MHOBOW

They demonstrated the existence of polarization splay in the layers driven by the local polar/chiral ordering, which leads to a polarization modulation. The splay of polarization is associated with defect lines necessary to fill the volume. The defect lines are the regions where the splay deformation of the in-plane orientation of the tilted optic axis changes its sign. There exists a layer expansion at these splay defects, which causes an undulation of the layers. This undulation leads to a non-centered rectangular 2D-lattice with lattice parameter *a* corresponding to the layer distance and parameter *b* corresponding to the undulation wavelength. On the basis of these results they proposed a polarization modulated/undulated layer structure associated with splay defects for such a mesophase. The proposed model is shown in figure **5.1**.

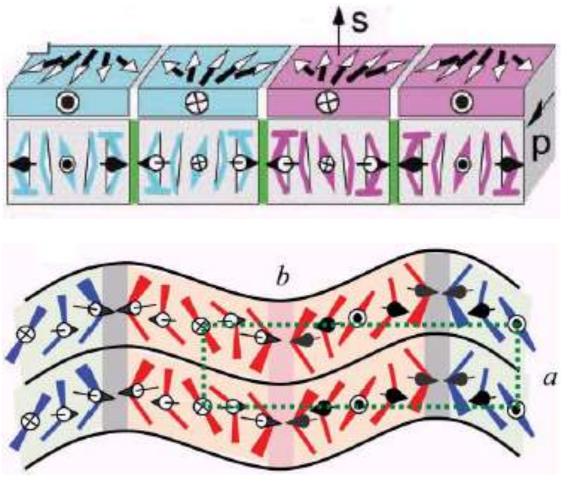

Figure 5.1: The proposed model of a polarization modulated/undulated layer stripe structure for the B_7 phase of compound MHOBOW [13].

Coleman *et al.* also carried out experiments on the mesophase exhibited by W1044, in which the B_7 phase was first observed [1]. XRD studies indicate an oblique 2D reciprocal lattice for this mesophase. They propose a polarization modulated and an interdigitated 2D lattice structure for this mesophase, which is the lattice structure of the B_1 phase. The authors suggest that in such a structure, the orientation frustration at the splay defect planes might be relieved by interdigitation of the layers, which accommodates the opposite orientation of the bent-core molecules on opposite sides of the defect lines.

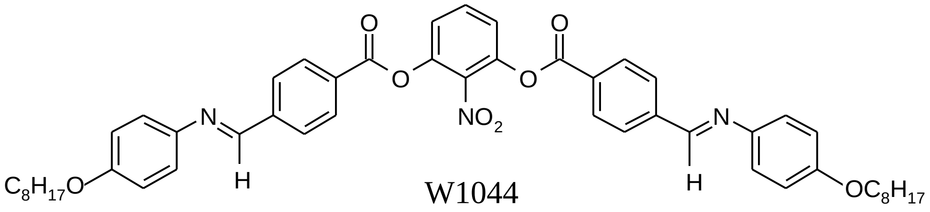

W1044

A schematic representation of the model proposed for compound W 1044 is shown in figure **5.2**.

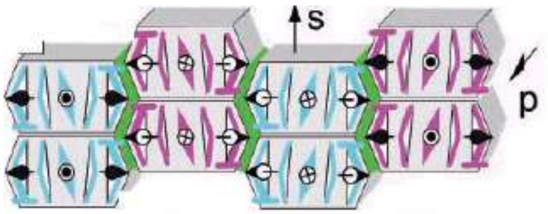

Figure 5.2: The proposed model for the B_7 mesophase of compound W 1044 [13].

However, it should be pointed out here that recently, Folcia *et al.* [14] also carried out a structural investigation of the B_7 phase exhibited by compound W 1044. They indexed the X-ray data to an oblique 2D lattice. Using additional information from optical second hormonic generation, they proposed several possible structural models based on molecular packing considerations. The deduced structures are closer to some columnar models proposed for the B_1 phase.

A couple of years ago, a series of Schiff's base esters derived from 2-nitroresorcinol in which, the direction of the Schiff's base units (azomethine linkage groups) is reversed with respect to the classical B_7 materials was reported [5] from our laboratory. Interestingly, a transition from a non-switchable B_7 mesophase at a higher temperature to an antiferroelectric sub-phase (B_{7AF1}) was observed in a couple of compounds belonging to this series. Except for these, there is no other report of a switchable B_7 phase in compounds derived from either 2-nitro- or 2-cyano-resorcinol.

In this chapter, the synthesis and mesomorphic properties of four new homologous series of Schiff's base five-ring BC compounds *viz.* **5.A**, **5.B**, **5.C** and **5.D** have been described. These compounds are derived from 2-cyano- and 2-nitro-resorcinol and contain terminal *n*-alkyl carboxylate groups. Compounds of series **5.A** and **5.B** (Part I) differ from those of **5.C** and **5.D** (Part II) with respect to the orientation of the azomethine linking group. In this study, the influence of orientation of the azomethine linkage group and the effect of the terminal carboxylate linking groups on the phase behaviour of the compounds derived from 2-cyano- and 2-nitro-resorcinol have been examined.

Part I

In this part, the synthesis and characterization of compounds belonging to series **5.A** and **5.B** are described. The compounds investigated have the general molecular structure shown below.

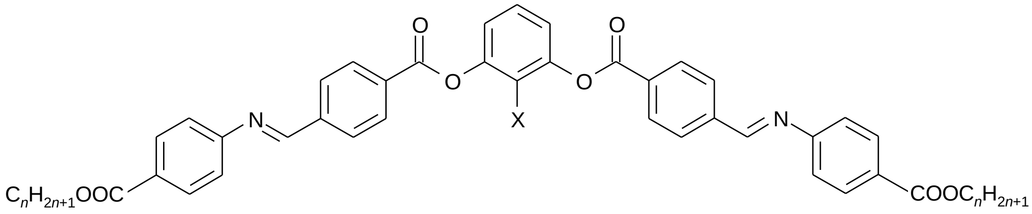

X=CN Series **5.A**

X=NO_2 Series **5.B**

Structure 5.1

Synthesis

2-Cyanoresorcinol was prepared from demethylation of commercially obtained 2,6-dimethoxybenzonitrile following a procedure described in the literature [3]. 2-Nitroresorcinol was obtained commercially and used without further purification. The five-ring symmetrical bent-core compounds were prepared by esterification of two equivalents of carboxylic acid, **5.a** with 2-cyanoresorcinol or 2-nitroresorcinol using *N*, *N′*-dicyclohexylcarbodiimide (DCC) as coupling reagent and 4-(*N*, *N*-dimethylamino)pyridine (DMAP) as catalyst in anhydrous dichloromethane at room temperature. A detailed procedure for the synthesis of 4-(4-*n*-alkyloxycarbonylphenyliminomethyl)benzoic acids, **5.a** is given in Chapter 4. The general synthetic pathway used to prepare the target compounds is depicted in scheme **5.1**.

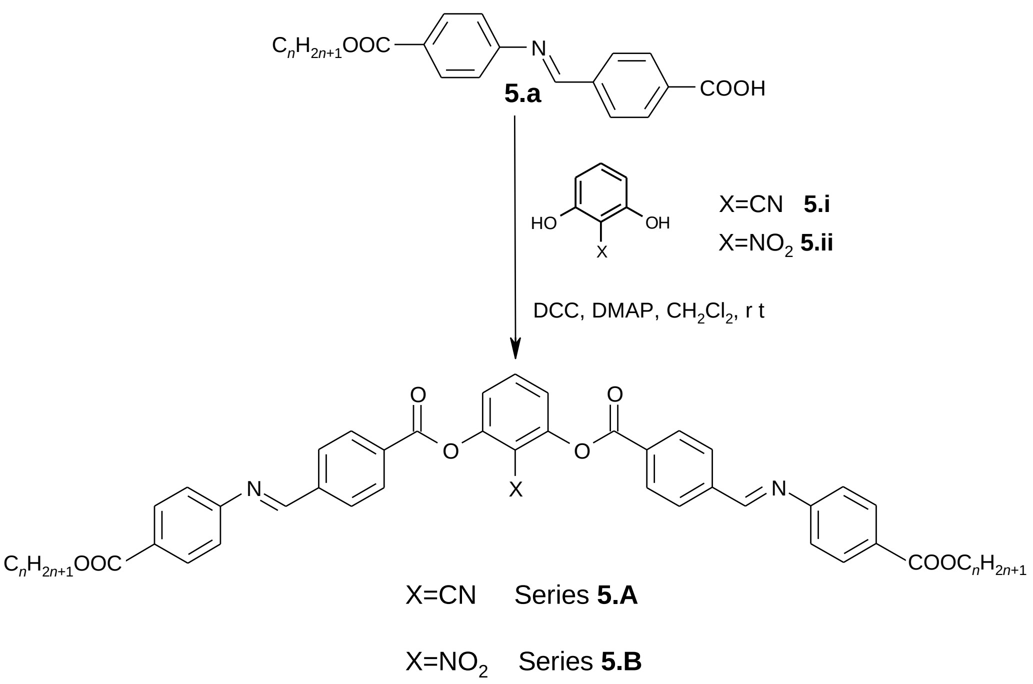

Scheme 5.1: **Synthetic pathway used for the preparation of strongly polar bent-core compounds 5.A and 5.B.**

Results and Discussion

The transition temperatures and the associated enthalpy values obtained for the compounds of series **5.A** are presented in table **5.1**. All the compounds of series **5.A** are dimorphic. The transition between the mesophases could be detected by calorimetry, although the enthalpy accompanying the transition is relatively small (1.5-4.5 kJ mol^{-1}). A DSC thermogram obtained for compound **5.A.2** is shown in figure **5.3**. Compounds **5.A.1-5.A.10** exhibit two mesophases, which are enantiotropic except compounds **5.A.7** and **5.A.8** in which the lower temperature (LT) mesophase is monotropic. It can be seen that on ascending the homologous series the thermal range of the higher temperature (HT) phase increases from 6.5˚C for compound **5.A.1** to 44˚C for compound **5.A.10** and, in contrast the thermal range of the lower temperature phase decreases from 32˚C for **5.A.1** to 10˚C for **5.A.10**. For compounds **5.A.9** and **5.A.10**, transition to the LT

Table 5.1: Transition temperatures (˚C) and the associated enthalpy values (kJ mol^{-1}, in italics) for compounds of series 5.A.

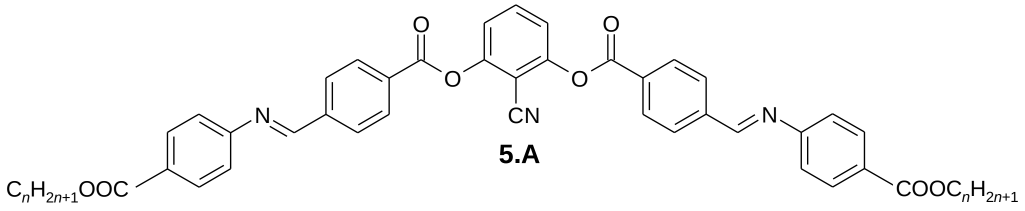

5.A

Compound	*n*	Cr		B$_{7X}$		B$_{7FE}$		I
5.A.1	6	.	121.0	.	153.0	.	159.5	.
			4.5		*4.5*		*24.2*	
5.A.2	7	.	120.0	.	143.0	.	161.5	.
			3.0		*3.5*		*27.0*	
5.A.3	8	.	113.0	.	137.0	.	163.5	.
			4.0		*3.0*		*25.5*	
5.A.4	9	.	115.5	.	132.0	.	164.5	.
			6.0		*3.0*		*27.0*	
5.A.5	10	.	118.0	.	129.0	.	165.5	.
			4.0		*4.0*		*22.0*	
5.A.6	11	.	117.5	.	125.3	.	166.0	.
			1.5		*3.5*		*26.5*	
5.A.7	12	.	131.5	(.	123.0)	.	166.0	.
			24.0		*4.0*		*27.0*	
5.A.8	14	.	125.5	(.	121.5)	.	164.5	.
			80.5		*4.0*		*24.5*	
5.A.9	16	.	108.0	.	119.5$^{\$}$	.	163.0	.
			75.5		*2.0*		*19.5*	
5.A.10	18	.	107.0	.	117.0$^{\$}$	.	161.0	.
			94.0		*1.5*		*22.0*	

Abbreviations for tables **5.1** and **5.2**: Cr-Crystalline phase; B$_7$ and B$_{7X}$ - Non-switchable mesophases with a two-dimensional lattice; B$_{7FE}$ -A mesophase with a two-dimensional lattice showing ferroelectric switching behaviour; I-Isotropic phase; () Monotropic transition; $^{\$}$ The phase transition was clearly observed only on cooling; *The compound has crystal-crystal transition and the enthalpy denoted is the sum of all such transitions; † Melting point was determined under a polarizing light microscope and enthalpy could not be determined.

phase could not be detected on heating the crystals, but was very clear on the cooling cycle from the HT phase. Microscopic observations also revealed a similar behaviour. A plot of the transition temperature as a function of the terminal chain length for this series is shown in figure **5.4**. It can be seen that smooth curve relationships are seen for both the clearing as well as the mesophase-mesophase transitions.

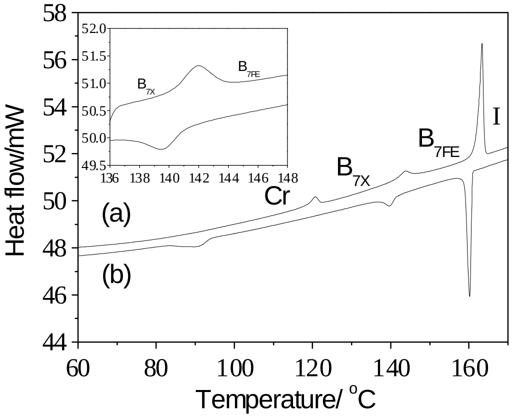

Figure 5.3:A DSC thermogram obtained for compound 5.A.2 at a scan rate of 5°C min^{-1}; (a) heating cycle; (b) cooling cycle. The inset shows an enlarged view of the mesophase to mesophase transition (scan rate 0.1°C).

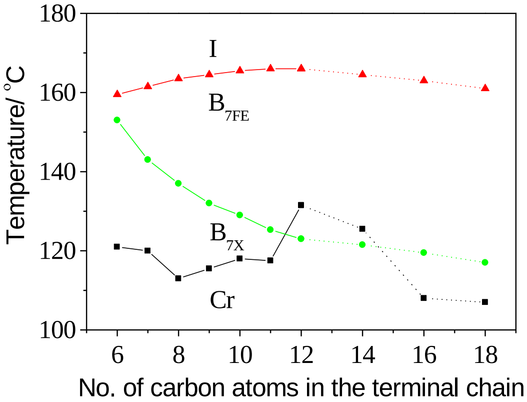

Figure 5.4: A plot of transition temperature *versus* the number of carbon atoms in the terminal *n*-alkyl chain for compounds of series 5.A.

All the homologues of this series exhibit similar optical textures when the respective isotropic liquids are cooled slowly, and they resemble those shown by the B_7 phase [1-5]. Helical filaments which are the characteristic feature of B_7 phase and other patterns obtained on slow cooling of the isotropic liquid of homologue **5.A.7** sandwiched between two glass plates are shown in figure **5.5**. These textural observations coupled with XRD studies (described later) indicate that the HT phase is indeed the classical B_7 phase. However, electro-optical studies (described later) show a ferroelectric behaviour and hence the symbol B_{7FE} was assigned for the HT phase. On cooling this phase further, a transition takes place at 123˚C accompanied by a change in the optical texture that is clearly visible (figure **5.6**) under the microscope. For example, the myelinic and the smooth fan-like patterns observed in the B_{7FE} phase (figure **5.6a** and **5.6c**) became completely dark on phase transition (figure **5.6b** and **5.6d**). Interestingly, the birefringence of the texture in other regions increased. The textural changes observed during this phase transition were the same irrespective of whether the glass plates were treated for homeotropic or planar alignment of the sample. This suggests that anchoring conditions do not have any influence on the texture of the mesophases. Since the XRD data of LT phase is almost the same as that of the B_{7FE} phase except for a few additional reflections, and the phase does not respond to an applied electric field this phase has been designated as B_{7X}. Similar textural change at the transition was observed for all the other homologues as well.

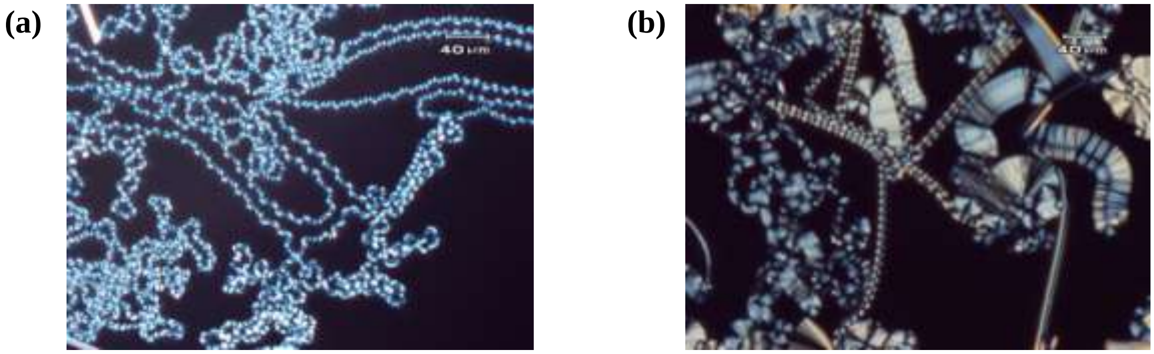

Figure 5.5: Textural photomicrographs obtained for the B_{7FE} phase of compound 5.A.7 in two different regions of the same sample, T=165˚C.

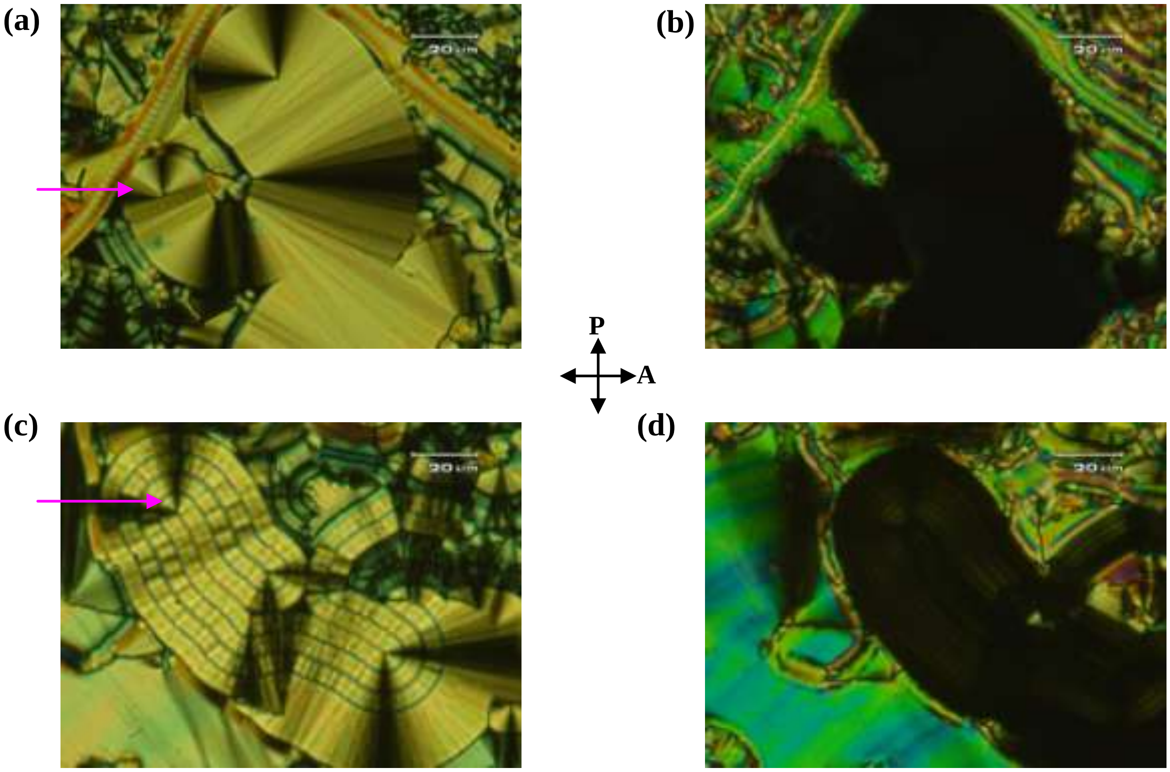

Figure 5.6: Photomicrographs obtained for compound 5.A.7 showing the textural change after the phase transition $B_{7FE} \rightarrow B_{7X}$ in a cell of thickness 5 μm treated for planar alignment; (a) and (c) at T=150°C; (b) and (d) at T=115°C (same region as in a and c respectively).

In complete contrast, the compounds of series **5.B**, which contain a nitro substituent in the angular position exhibit only one mesophase. The transition temperatures and the associated enthalpy values obtained for the compounds of series **5.B** are presented in table **5.2**. Surprisingly, the melting point of compounds **5.B.3**, **5.B.5** and **5.B.7** could not be accurately determined from DSC measurements. However, melting point could be detected under a polarizing light microscope. A plot of transition temperature as a function of the number of carbon atoms in the terminal *n*-alkyl chain for the compounds of series **5.B** is shown in figure **5.7**. It is seen that the clearing temperatures fall on a smooth curve. These compounds also exhibit helical filaments and other two-dimensional patterns that are normally associated with a B_7 phase. A couple of such textures obtained for the mesophase of compound **5.B.6** are shown in figure **5.8**. Interestingly,

Table 5.2: Transition temperatures (˚C) and the associated enthalpy values (kJ mol^{-1}, in italics) for compounds of series 5.B.

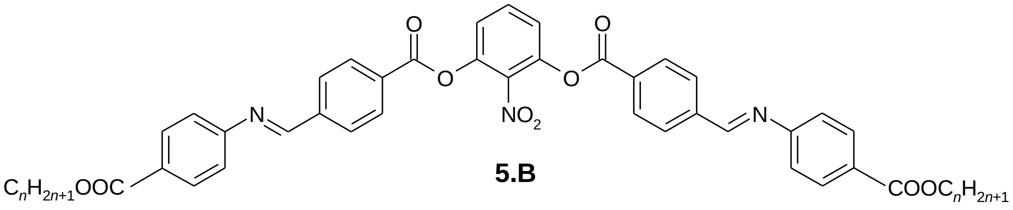

5.B

Compound	*n*	Cr		B_{7FE}		I
5.B.1	8	.	85.5	.	139.0	.
			8.3		*24.0*	
5.B.2	9	.	93.5	.	142.5	.
			10.5		*23.0*	
5.B.3	10	.	90.0†	.	146.0	.
					24.0	
5.B.4	11	.	89.0	.	147.5	.
			39.0		*20.5*	
5.B.5	12	.	87.5†	.	148.0	.
					20.5	
5.B.6	14	.	83.0	.	148.5	.
			47.0		*25.0*	
5.B.7	16	.	98.0†	.	147.5	.
					22.5	
5.B.8	18	.	81.5	.	146.0	.
			33.5		*19.0*	

Abbreviations: See table **5.1**

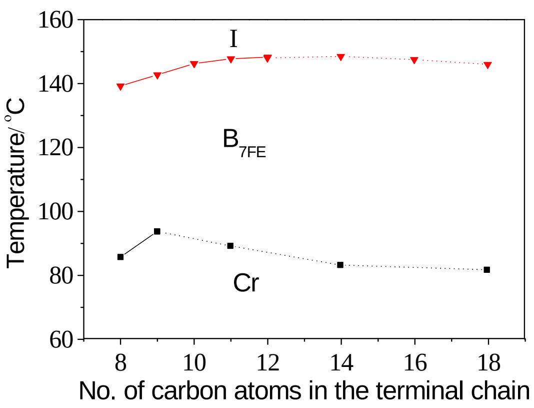

Figure 5.7: A plot of transition temperature *versus* the number of carbon atoms in the terminal *n*-alkyl chain for compounds of series 5.B.

compounds **5.B.1**-**5.B.5** also exhibit a texture composed of chiral domains of opposite handedness. This mesophase has been identified as a B_{7FE} phase on the basis of textural observations, XRD studies and electro-optical studies.

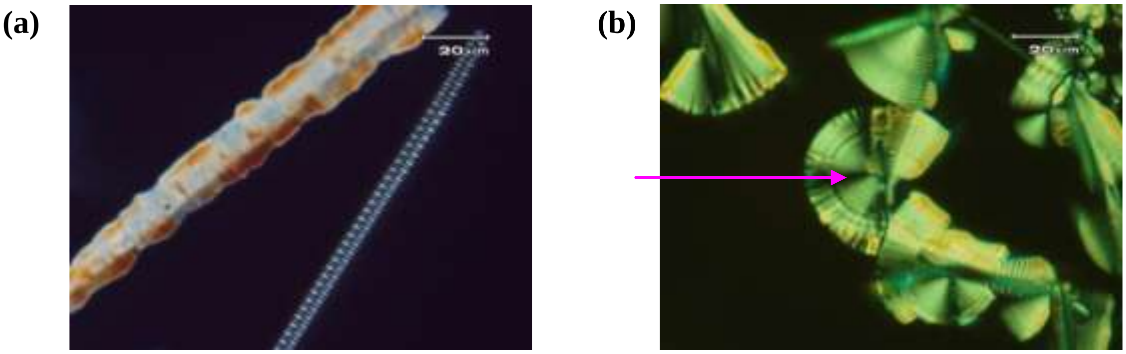

Figure 5.8: Photomicrographs of the textures obtained for the B_{7FE} mesophase of compound 5.B.6, T=147.3°C.

It is interesting to point out here that the extinction cross obtained in the partial circular domains as well as in the myelinic-like texture (indicated by an arrow in figure **5.6a**, **5.6c** and figure **5.8b**) are parallel to the direction of crossed polarizers. This is similar to the previous observations of the B_7 phase exhibited by strongly polar compounds [1-5].

XRD measurements were carried out on powder samples of selected compounds from series **5.A** and series **5.B** in order to obtain information on the phase structure. XRD pattern of the HT (B_{7FE}) phase of compound **5.A.2** showed several incommensurate Bragg reflections in the small angle region. This suggests a non-layered structure for the mesophase. A medium angle reflection was also observed at around 7.7Å. This is a characteristic peak seen for the B_7 mesophase exhibited by all the compounds derived from 2-cyano-, 2-nitro- or 5-fluoro-resorcinol [1-6]. A diffuse reflection was observed in the wide-angle region at around 4.2Å, indicating the fluidity of the phase. When the sample was cooled to B_{7X} phase, the reflections obtained in the B_{7FE} phase were retained. However, additional reflections were also seen which pointed towards a more ordered mesophase. The X-ray diffractogram obtained in the small angle region of both the B_{7FE} and B_{7X} phases of compounds **5.A.2** and **5.A.7** are shown in figure **5.9a**. The additional reflections obtained in the B_{7X} phase are shown by arrows in this figure. It is interesting to note from this plot that, the small angle reflections in the B_{7X} phase have shifted to slightly lower values (increase in *d*), while the medium angle reflection has shifted to a higher value (decrease in *d*). It has been pointed out [12] that, the distance corresponding to the medium angle reflection (*d*- ~ 7-8Å) is in the range of typical value of face-to-face packed dimers. Remarkably, all compounds forming B_7 phase have highly polar substituents, like CN, NO_2 and F at the central phenyl ring of the bent unit. Electron deficient compounds are known to form face-to-face aggregates, where by the planes of the aromatics are shifted with respect to each other [15]. It was suggested [12] that if such a face-to-face packing takes place in the B_7 phase, then the medium angle reflection might indicate some order between these dimers. In the absence of high resolution XRD data, it would be difficult to interpret the observations.

Although an interdigitated two-dimensional smectic layer structure has been proposed for the B_7 phase of a 2-cyano substituted compound on the basis of synchrotron X-ray diffraction techniques [13, 16], the precise structure of the phase is not yet clear. Therefore it is rather difficult to propose a structure for the phase, which exists below the B_{7FE} phase. Since there are a few additional reflections in the XRD pattern as compared to the standard B_7 mesophase [1], the symbol B_{7X} has been assigned for the LT phase. Similar XRD patterns were obtained for the other homologues of series **5.A**. The XRD patterns obtained for the compounds of series **5.B** are also similar to the B_{7FE} phase and a typical angular intensity profile obtained for compound **5.B.6** is shown in figure **5.9b**.

In order to investigate the polar properties of the mesophase, electric field experiments were carried out on representative compounds from the two series. A sample of compound **5.A.7** in the isotropic state was filled into an ITO coated cell of thickness 13.4 μm through capillary action. The sample was cooled from the isotropic state to the mesophase (T=140˚C) and a triangular-wave voltage was applied and this was increased slowly. At a voltage of $400V_{pp}$ and a frequency of 50 Hz, a small hump was observed in the current response trace, which became a prominent peak on reducing the frequency (10 Hz). The single peak obtained persisted even on reducing the frequency down to 0.1 Hz, indicating a ferroelectric behaviour for the mesophase. The ferroelectric nature was further supported by the current response of the mesophase under a modified triangular-wave with a plateau at 0V, during which also only one peak was observed per each half cycle. The peak obtained in the mesophase disappeared on going to the isotropic phase thus ruling out the possibility of ionic contribution. The current response traces obtained by the application of a triangular-wave voltage of 400V$_{PP}$, 10 Hz and modified triangular-wave voltage of 400V$_{PP}$, 4 Hz are given in figure **5.10a** and **b** respectively. The polarization value estimated

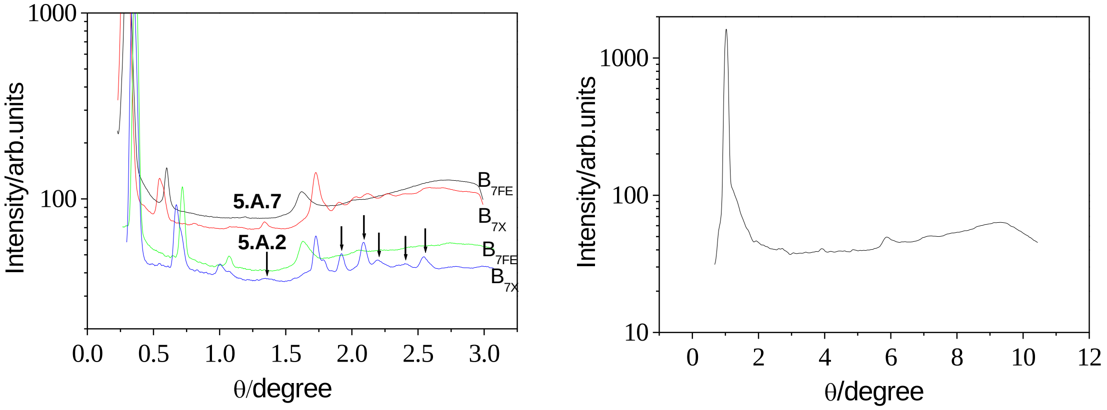

(a) **(b)**

Figure 5.9: Plots of intensity *versus* Bragg angle (θ) obtained from the X-ray diffraction pattern. (a) Compound 5.A.2 at T=150˚C (B_{7FE}), 130˚C (B_{7X}) and compound 5.A.7 at T=140˚C (B_{7FE}), 112˚C (B_{7X}); (b) compound 5.B.6 at T=120˚C (B_{7FE}).

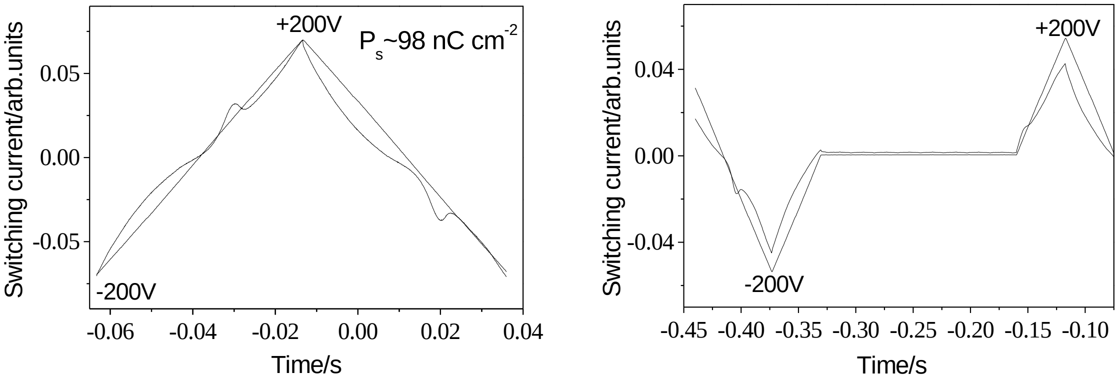

(a) **(b)**

Figure 5.10: Switching current response trace obtained for the B_{7FE} phase of compound 5.A.7 at 140˚C in an ITO coated cell of thickness 13.4 μm by applying (a) triangular-wave voltage, 400V$_{pp}$, 10Hz and (b) modified triangular-wave voltage, 400V$_{pp}$, 4Hz.

from this trace is about 98 nC cm^{-2}. Hence, the symbol B_{7FE} was assigned for this HT phase. On cooling the mesophase further under the electric field (400V$_{pp}$, 10 Hz) there was a gradual decrease in the peak size, which completely disappeared at 122˚C (B_{7X} phase). This indicates that the B_{7X} phase does not respond to the applied electric field.

The optical response of the mesophase on application of an electric field was observed under a polarizing microscope. In the B_{7FE} phase smooth fans as well as circular domains were seen in which the extinction brushes are oriented along the crossed polarizers. This indicates an anticlinic tilt of the molecules in the mesophase. The texture remained the same on reversing the polarity of the applied field as well as on turning off, except for a slight variation in the birefringence. These observations suggest a racemic ferroelectric structure for the mesophase. On transition to the LT phase, a slight change in the texture was observed accompanied by a colour change. However, the orientation of the extinction brushes in the circular domains remained the same as in B_{7FE} phase. The photomicrographs obtained under these conditions are shown in figure **5.11**.

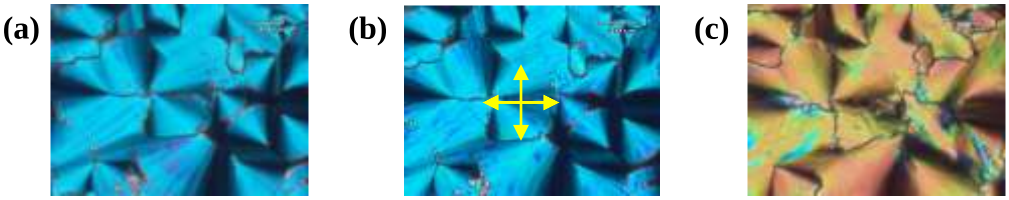

Figure 5.11: Photomicrographs obtained for the mesophase of compound 5.A.7 on application of triangular-wave electric field. (a) 400V$_{pp}$, 10Hz, 140˚C; (b) on switching off the field, 140˚C; (c) 400V$_{pp}$, 10 Hz, 120˚C.

The mesophase exhibited by compounds of series **5.B** was also found to be polar and shows ferroelectric switching characteristics. For example, the polarization value estimated from the current response trace obtained for compound **5.B.2** is about 184 nC cm^{-2}.

It is appropriate to mention here that, until now there are only two examples of switchable B_7 phase obtained from compounds whose central phenyl unit contains a highly polar substituent. These are five-ring Schiff's base bent-core compounds derived from 2-nitroresorcinol in which a transition from a non-switchable B_7 mesophase at a higher temperature to an antiferroelectric sub-phase (B_{7AF1}) was observed [5] and 5-fluororesorcinol, which exhibit an antiferroelectric SmCP phase at higher temperature and a ferroelectric B_7 phase at a lower temperature [6]. However, the present work described here is the first example of a B_7 phase exhibited by bent-core compounds derived from 2-cyanoresorcinol which show ferroelectric characteristics to an applied electric filed and dimorphism as well.

Part II

In this part, the synthesis and mesomorphic properties of two homologous series of compounds (series **5.C** and **5.D**) are described. The compounds investigated have the general molecular structure shown below.

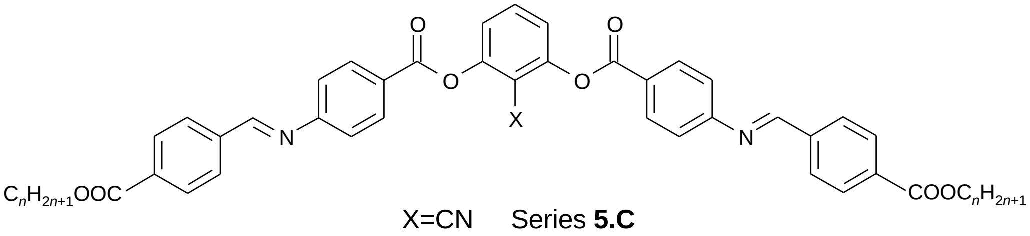

X=CN Series **5.C**

X=NO_2 Series **5.D**

Structure 5.2

Synthesis

The new symmetrical bent-core compounds were prepared following a pathway shown in scheme **5.2**. A detailed procedure for the synthesis of 4-(4-*n*-alkyloxycarbonylbenzylidene-amino)benzoic acid is given in Chapter 4. The five-ring bent-core compounds were prepared by esterification of this acid with a 2-substituted resorcinol using DCC as a dehydrating agent and DMAP as a catalyst in dry dichloromethane.

Results and discussion

Both the series of compounds are symmetrical about the central phenyl unit and contain five rings in the core. The two terminal chains are incorporated as esters in contrast to the usual *n*-alkyl or *n*-alkoxy chains. The compounds of series **5.C** are derived from 2-cyanoresorcinol. The transition temperatures and the associated enthalpy values obtained for this series of compounds are summarized in table **5.3**. As can be seen in table **5.3**, all the six homologues are enantiotropic mesomorphic with compound **5.C.4** having the largest thermal range of about 50.5˚C. All these compounds exhibit a variety of textures, which are typical for a B_7 phase [1], and one of the characteristic textures is the formation of helical patterns. For example, when a sample of compound **5.C.4** is cooled slowly from the isotropic phase, helical texture develops and photomicrographs of these are shown in figure **5.12**. In addition, a variety of other fascinating patterns are also formed and three of these are shown in figure **5.13**.

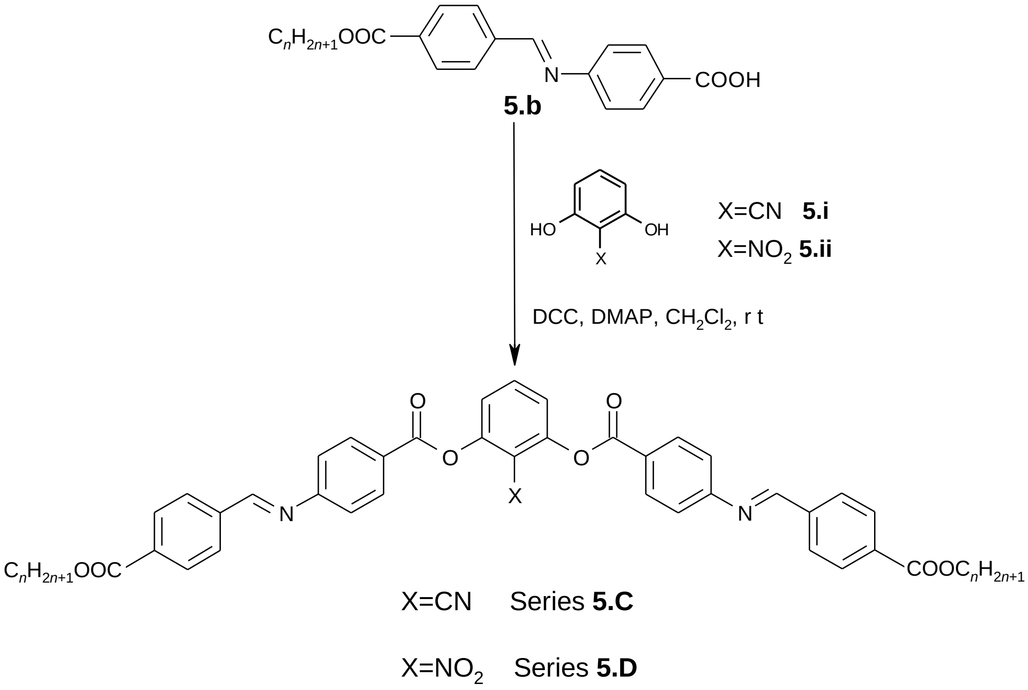

Scheme 5.2: Synthetic route employed for the preparation of the bent-core compounds belonging to series 5.C and 5.D.

In fact, several compounds derived from 2-cyanoresorcinol and exhibiting the B_7 phase have been reported [2-4] which show several beautiful textures. On the basis of the textural observations, XRD studies and electro-optical investigations (does not respond to an applied electric field), the mesophase exhibited by compounds **5.C.1-6** has been characterized as B_7. A plot of the transition temperature as a function of the number of carbon atoms in the terminal chain is shown in figure **5.14**. The $B_7 \rightarrow I$ transition points fall on a smooth curve, which is again typical for this type of transition [2-4].

Table 5.3: Transition temperatures (˚C) and the associated enthalpy values (kJ mol^{-1}, in italics) for the compounds of series 5.C.

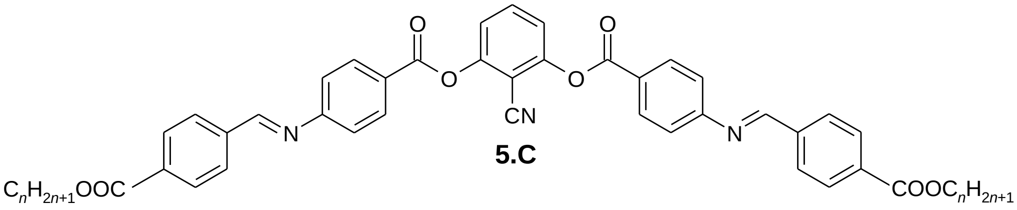

5.C

Compound	*n*	Cr		B_7		I
5.C.1	10	.	123.5*	.	144.0	.
			45.6		*26.3*	
5.C.2	11	.	128.5*	.	145.5	.
			34.0		*26.0*	
5.C.3	12	.	114.0*	.	144.5	.
			39.5		*21.0*	
5.C.4	14	.	96.5*	.	147.0	.
			56.4		*24.1*	
5.C.5	16	.	103.0*	.	147.0	.
			64.0		*23.9*	
5.C.6	18	.	107.5	.	147.5	.
			72.7		*22.0*	

Abbreviations: see table **5.1**

The compounds of series **5.D** are derived from 2-nitroresorcinol. The transition temperatures and the associated enthalpy values obtained for the compounds of this series are given in table **5.4**. All the six homologues of this series are enantiotropic mesomorphic. Compound **5.D.5** has a fairly wide thermal range of 54˚C for the mesophase. Surprisingly, compounds **5.D.1-3** exhibit a dark texture on cooling from the isotropic phase. However, domains of opposite handedness could be seen by rotating (~5˚) either the polarizer or analyzer. Such chiral domains of opposite handedness were first reported by Thisayukta *et al.*[17, 18] and Heppke *et al.* [8] and later such domains have been observed in number of other systems [6, 19-27]. It is noteworthy to point out here that, most of the phases exhibiting this dark texture have $SmCP_{A/FE}$

phase structure. However, Pelzl *et al*. have reported [6] a texture with chiral domains of opposite handedness for the B_7 mesophase which appear below a higher temperature $SmCP_A$ phase. The chiral domains formed in the higher temperature $SmCP_A$ phase are retained in the lower temperature B_7 mesophase. Such chiral domains observed in compounds **5.D.1-3** is the first example of such a texture for a B_7 mesophase appearing directly from the isotropic phase.

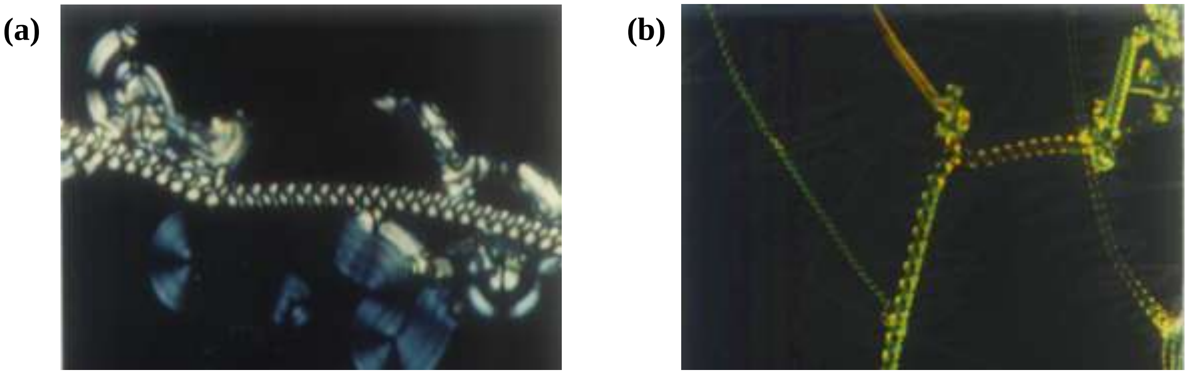

Figure 5.12: (a) and (b), Photomicrographs of the helical patterns forming on cooling the isotropic phase of compound 5.C.4,T=145.5˚C.

Photomicrographs showing the chiral domains of opposite handedness obtained for the B_7 mesophase of compound **5.D.2** is shown in figure **5.15a** and **b**. These domains are fairly large and the formation of these domains depends on the rate of cooling. In addition, compounds **5.D.4-5.D.6** show filamentary texture when their isotropic liquids are cooled slowly. A typical texture obtained on cooling the isotropic liquid of compound **5.D.4** is shown in figure **5.16**.

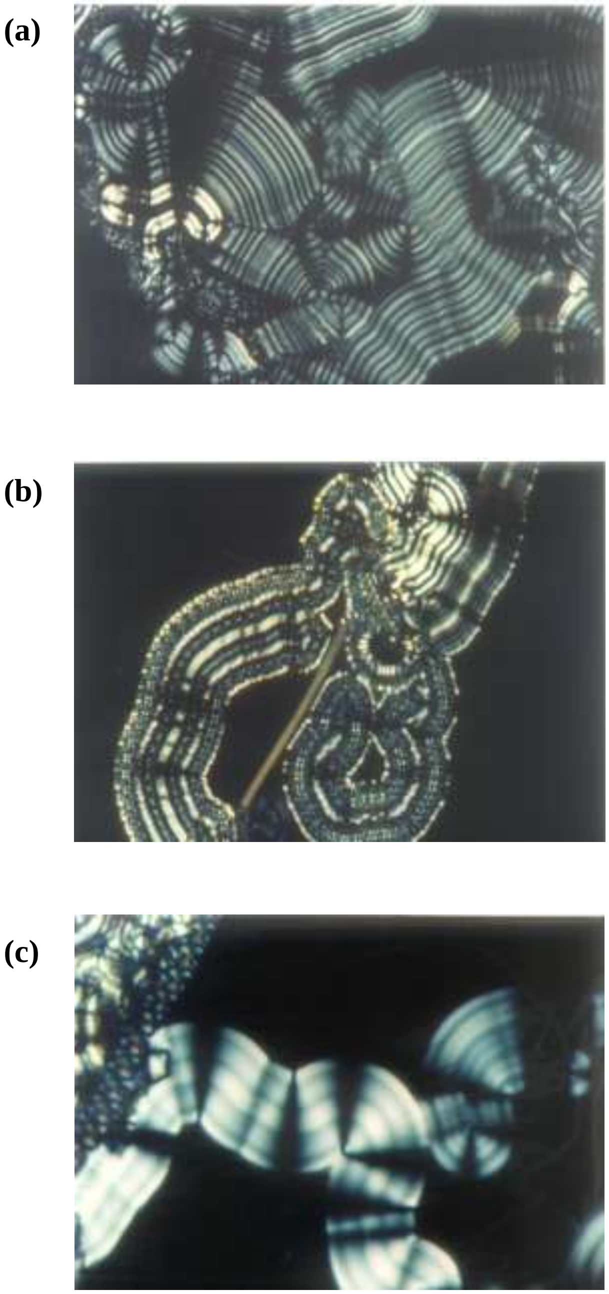

Figure 5.13: (a), (b) and (c), Various fascinating patterns of the B_7 phase of compound 5.C.4 obtained on slow cooling of the isotropic phase, T=145.5˚C.

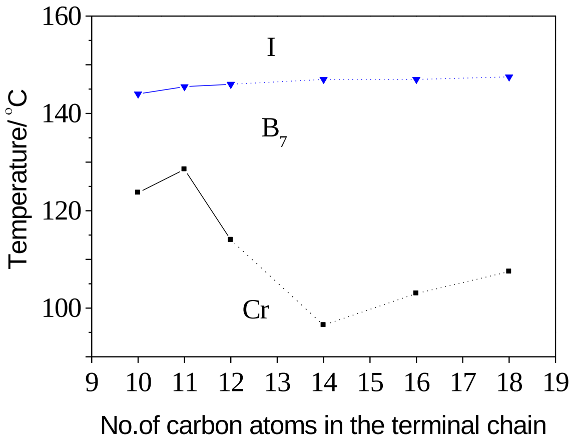

Figure 5.14: A plot of transition temperature as a function of the number of carbon atoms in the terminal chain for compounds of series 5.C.

Table 5.4: Transition temperatures (°C) and the associated enthalpy values (kJ mol^{-1}, in italics) for the compounds of series 5.D.

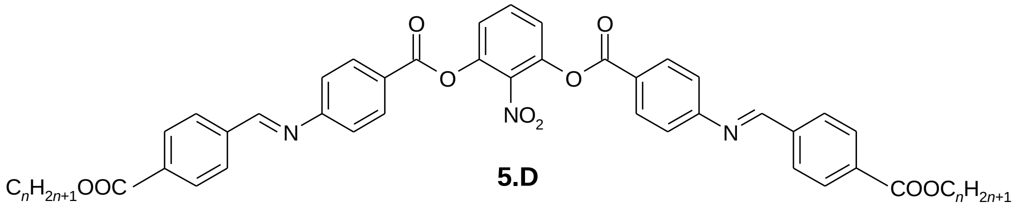

5.D

Compound	*n*	Cr		B_7		I
5.D.1	10	.	106.5*	.	143.0	.
			18.0		*32.0*	
5.D.2	11	.	101.0*	.	143.5	.
			43.5		*33.0*	
5.D.3	12	.	91.0	.	143.5	.
			4.5		*28.5*	
5.D.4	14	.	93.0*	.	143.5	.
			55.2		*29.0*	
5.D.5	16	.	89.5*	.	143.5	.
			34.8		*27.4*	
5.D.6	18	.	92.0*	.	143.0	.
			70.9		*26.8*	

Abbreviations: See table **5.1**

This again is rather an unusual observation. Such filamentary growth pattern was previously observed [28] at the isotropic to SmCP$_A$ phase transition in a number of unsymmetrical bent-core compounds derived from 3-hydroxybenzoic acid. It should be noted that helical filaments and other two-dimensional patterns, normally seen for the B$_7$ phase, could also be observed on very slow cooling of the isotropic liquid. However, the mesophases of all the six compounds show the same XRD pattern and also do not switch electro-optically. A plot of the transition temperature *versus* the number of carbon atoms in the terminal chain for this series is shown in figure **5.17**. The clearing temperatures follow a smooth curve, as seen for the compounds of series **5.C**.

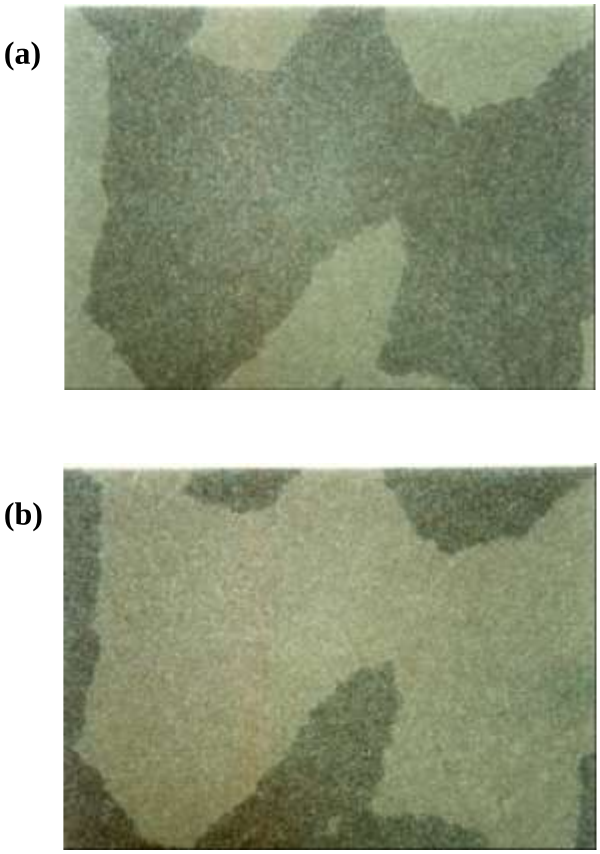

Figure 5.15: Microscopic texture of the B$_7$ phase of compound 5.D.2 obtained on rotating the polarizer by a) +5° and b) -5° from its crossed position, T=140°C.

Figure 5.16: Photomicrograph showing the filamentary texture for the B_7 phase of compound 5.D.4, T=141.5˚C.

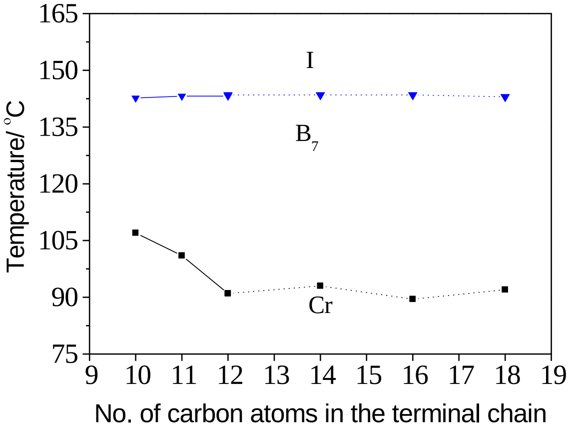

Figure 5.17: A plot of transition temperature as a function of the number of carbon atoms in the terminal chain for compounds of series 5.D.

XRD experiments were carried out on non-oriented mesophases of compounds belonging to series **5.C** and **5.D**. The data obtained are summarized in table **5.5**. The X-ray diffractograms of the mesophase of all these compounds are quite similar. For example, the XRD pattern of compound **5.D.4** showed several reflections in the small angle region with *d* spacings 43.5Å,

Table 5.5: Layer spacing (Å) from XRD measurements of the mesophase of compounds belonging to series 5.C and 5.D.

Compound	*d* spacing /Å	Temperature/˚C
5.C.1	37.4, 19.1, 7.7	135
5.C.4	43.0, 21.8, 7.6	125
5.C.6	46.8, 16.1, 7.7	125
5.D.1	39.0, 7.7	130
5.D.4	43.5, 32.2, 11.3, 9.5, 7.5	135
5.D.6	48.8, 24.7, 7.5	125

32.2Å, 11.3Å, 9.5Å and 7.5Å, ruling out the possibility of a simple layer structure. The X-ray angular intensity profile obtained for the mesophase of this compound is shown in figure **5.18**. The pattern has very close similarity to that of the B_7 phase reported earlier [1-5]. Similar patterns

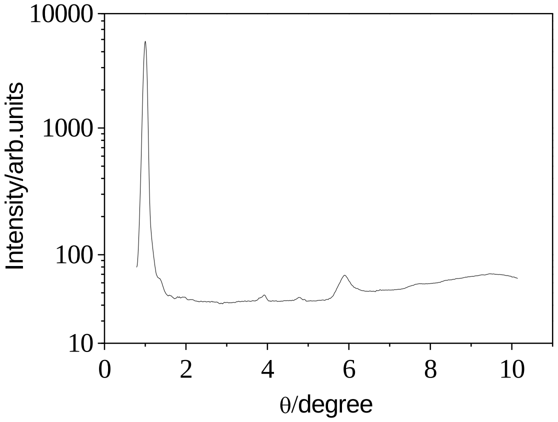

Figure 5.18: X-Ray angular intensity profile obtained for the B_7 mesophase of compound 5.D.4, T=135˚C.

were obtained for all the other compounds of the two series. A reflection centered around 7.5Å was observed in all of these, which is a characteristic reflection seen in the B_7 phase of all compounds derived from 2-cyano- and 2-nitro-resorcinol. A diffuse wide-angle reflection was observed around 4.2Å indicating a liquid-like in-plane order.

Electric field experiments were carried out on representative compounds belonging to both the homologous series. ITO coated transparent cells, which were treated for planar alignment (EHC, Japan) with a cell gap of 8 μm were used for the experiments. No electro-optical response was observed up to a triangular voltage of $50V\mu m^{-1}$ over the entire mesophase range.

Effect of orientation of azomethine linkage group

A comparison was made between the compounds of two series **5.A** and **5.B** and the compounds of series **5.C** and **5.D** (figure **5.19**), which differ by the way in which the azomethine linking group is connected.

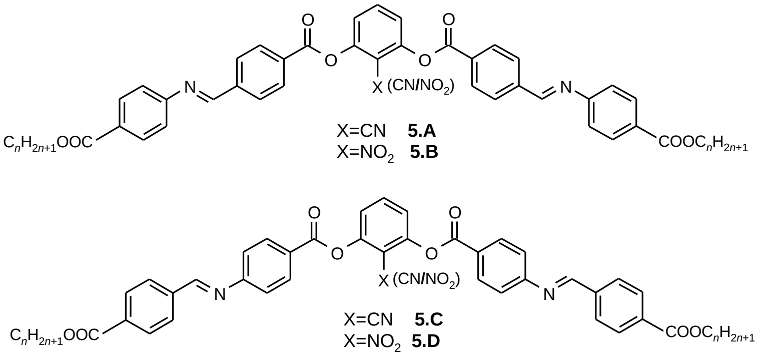

Figure 5.19: Chemical structure of the compounds used for comparison.

Interestingly, two mesophases were observed for all the compounds of series **5.A** while compounds of series **5.C** exhibited only one phase. Even more interestingly, of the two phases obtained for the compounds of series **5.A**, the higher temperature phase (B_{7FE}) responds to an applied electric field. This is in complete contrast to the compounds of series **5.C**, which are monomorphic and exhibit a non-switchable B_7 phase. A comparison of the transition temperature *versus* the number of carbon atoms in the terminal chain and the thermal range of the mesophases for the compounds of series **5.A** and series **5.C** is shown in figure **5.20a** as a bar diagram. It can be seen from the graph that in series **5.A**, the clearing transition temperatures are increased by about 20˚C in addition to inducing an additional switchable phase.

A similar comparison was made between the compounds of series **5.B** and the analogous compounds with the reversal of azomethine linking group belonging to series **5.D**. In this case also clearing transition temperatures of the B_{7FE} phase of compounds of series **5.B** are enhanced, but the increase in the temperature is relatively small and is only about 3-5˚C. However, the melting points have been reduced by about 10˚C resulting in an increase in the thermal range of the B_{7FE} phase. The observed differences between these two series of compounds are shown in figure **5.20b** as a bar diagram. Further, the mesophase (B_{7FE}) of compounds of series **5.B** exhibits ferroelectric characteristics, while B_7 phase exhibited by compounds **5.D** is non-switchable. These observations clearly demonstrate the profound change induced as a result of a small change in the form of reversal of the azomethine linking group.

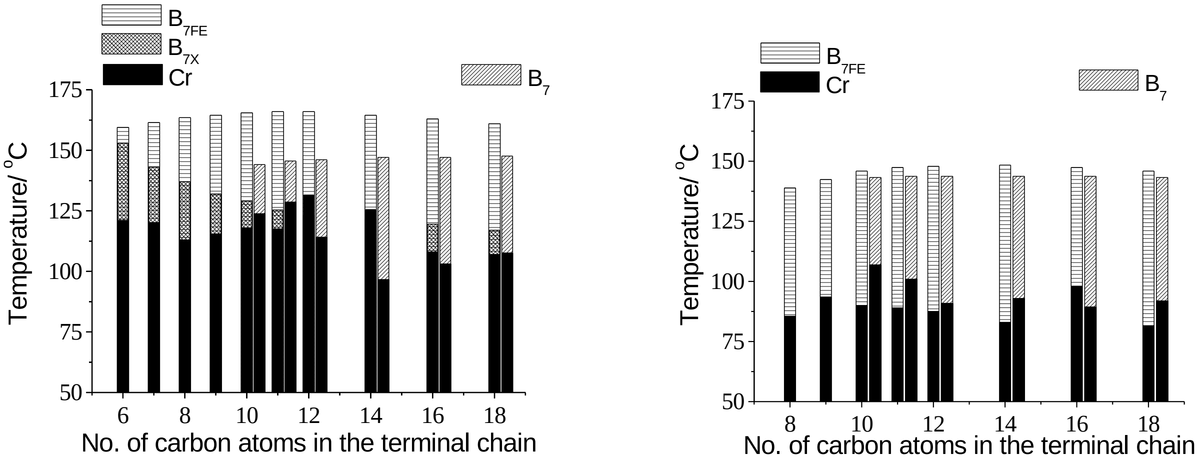

(a) **(b)**

Figure 5.20: A bar diagram showing a comparison of transition temperature *versus* the number of carbon atoms in the terminal chain and the thermal range of the mesophases. (a) Series 5.A (left column) and series 5.C (right column); (b) series 5.B (left column) and series 5.D (right column).

Effect of terminal linking group

A majority of the bent-core compounds contain *n*-alkyl or *n*-alkoxy chains directly attached to the phenyl ring in the terminal positions whereas in the present series of compounds *n*-alkyl chain is attached to a carboxyl group. This small change induces a drastic change in the mesomorphic behaviour as described below.

A comparison (figure **5.21**) of the mesomorphic properties of compounds of series **5.A** with the analogous compounds having terminal *n*-alkoxy chains [4] (series **E**) indicates the following interesting features.

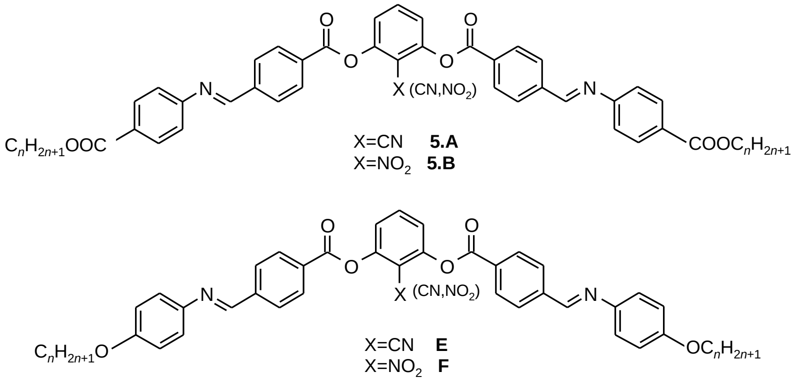

Figure 5.21:Chemical structure of the compounds used for comparison.

Two mesophases are observed for all the compounds of series **5.A**. The higher temperature phase (B_{7FE}) shows ferroelectric response to an applied electric field whereas the lower temperature phase is non-switchable. The compounds, 2-cyano-1,3-phenylene bis [4-(4-*n*-alkoxyphenyliminomethyl)benzoates] (series **E**) are monomorphic and the B_7 phase exhibited by them do not show any response to an applied electric field at least upto 40 Vμm^{-1} [4]. Further, melting points and clearing temperatures of compounds of series **5.A** are reduced considerably. An increase in the thermal range of switchable (B_{7FE}) phase has also been observed. A comparative plot of transition temperature as a function of the number of carbon atoms in the terminal chain and the thermal range of the mesophases is shown as a bar diagram in figure **5.22a**.

A similar comparative study between the compounds of series **5.B** and the compounds with the same core but terminal *n*-alkoxy chains [1] (series **F**) again indicates a reduction in melting points as well clearing temperatures. However, the decrease in the melting points is relatively small. The compounds of series **5.B** exhibit a switchable B$_7$ phase (B$_{7FE}$), while the B$_7$ phase exhibited by compounds of series **F** is non-switchable [1]. A comparative plot of the transition temperature as a function of the number of carbon atoms and the thermal range of the mesophases for the compounds of series **5.B** and those of series **F** is shown in figure **5.22b**.

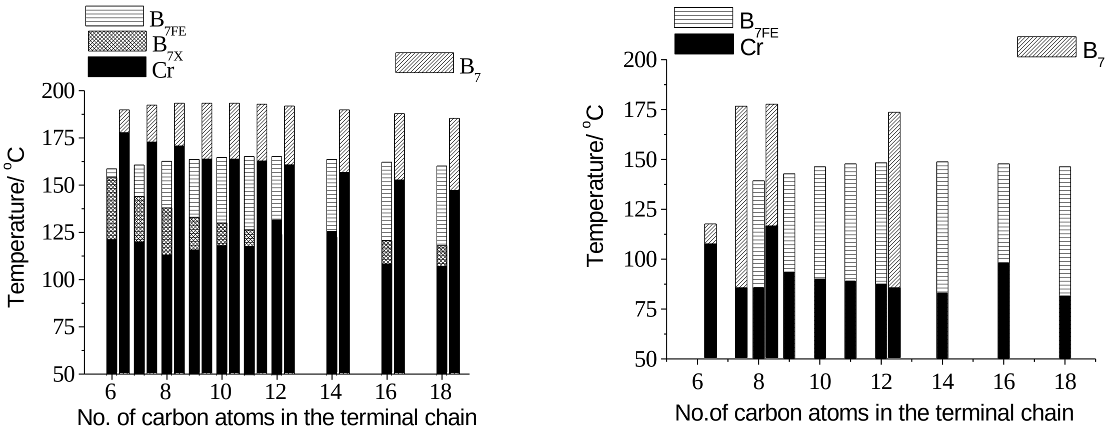

(a) **(b)**

Figure 5.22: A bar diagram showing a comparison of transition temperature as a function of number of carbon atoms in the terminal chain and the thermal range of the mesophases. (a) Compounds of series 5.A (left column) and those of series E [4] (right column); (b) compounds of series 5.B (left column) and standard B$_7$ material (series F) [1] (right column).

Conclusions

Four novel series of achiral five-ring bent-core compounds derived from 2-cyano- and 2-nitro-resorcinol containing *n*-alkyl carboxylate groups in the terminal positions were synthesized and their mesomorphic properties investigated. These are Schiff's base ester compounds and the compounds of series **5.A** and **5.B** differ from the compounds of series **5.C** and **5.D** only in the orientation of the azomethine linking group. All the compounds of series **5.A** and **5.B** exhibit a B$_7$ phase, which show ferroelectric switching characteristics. In addition, homologues of 2-cyano-substituted compounds displayed a transition from a switchable (B$_{7FE}$) phase to a non-switchable

(B_{7X}) mesophase as the temperature was lowered. This is the first observation of dimorphism in BC compounds, in which the higher temperature phase (B_{7FE}) is electro-optically switchable and the lower temperature phase (B_{7X}) is non-switchable, and the compounds are derived from 2-cyanoresorcinol. In addition, the B_7 phase observed in compounds derived from 2-nitroresorcinol is monomorphic and responds to an applied electric field and this phase and the higher temperature phase of cyano substituted compounds are the same. The compounds of series **5.C** and **5.D** exhibit a non-switchable B_7 mesophase. The mesophases exhibited by all these compounds show the medium angle reflection in the XRD pattern displayed by the B_7 mesophase of original 2-nitro substituted resorcinol derivatives.

Synthesis

A detailed procedure for the synthesis of 4-(4-*n*-alkyloxycarbonylphenyliminomethyl)benzoic acids, **5.a** and 4-(4-*n*-alkyloxycarbonylbenzylideneamino)benzoic acids, **5.b** and the corresponding spectral and analytical data obtained for these compounds are given in Chapter 4.

2-Cyano-1, 3-phenylene bis [4-(4-*n*-hexyloxycarbonylphenyliminomethyl)benzoate], 5.A.1

A mixture of 4-(4-*n*-hexyloxycarbonylphenyliminomethyl)benzoic acid, **5.a** (0.5g, 1.41 mmol), 2-cyanoresorcinol, **5.i** (0.07g, 0.57 mmol), DCC (0.25g, 1.55 mmol) and a catalytic amount of DMAP was stirred at room temperature for 12 hours. The precipitated urea was filtered off and washed thoroughly with chloroform. The filtrate was concentrated and the material obtained was crystallized several times using a mixture of chloroform and acetonitrile. Yield 0.4 g (73%), m. p. 121.0˚C. ν_{max}: 2922, 2852, 2667, 1745, 1739, 1737, 1712, 1461, 1377, 1280 cm^{-1}; δ_H: 8.55 (s, 2H, 2 × -CH═N-), 8.38 (d, ^3J 8.32 Hz, 4H, Ar-H), 8.11 (d, ^3J 8.4 Hz, 4H, Ar-H), 8.09 (d, ^3J 8.32 Hz, 4H, Ar-H), 7.77 (t, ^3J 8.4 Hz, 1H, Ar-H), 7.49 (d, ^3J 8.4 Hz, 2H, Ar-H), 7.26 (d, ^3J 8.4 Hz, 4H, Ar-H), 4.33 (t, ^3J 6.64 Hz, 4H, 2× Ar-COO-CH_2-), 1.82-1.75 (quin, ^3J 6.68 Hz, 4H, 2 × Ar-COO-CH_2-$\underline{CH_2}$-), 1.46-1.28 (m, 12H, 2 × $(-CH_2-)_3$), 0.88 (t, ^3J 6.48 Hz, 6H, 2 × -CH_3); $C_{49}H_{47}N_3O_8$ requires C 73.03, H 5.88, N 5.21; found C 72.98, H 5.75, N 4.79 %.

2-Cyano-1, 3-phenylene bis [4-(4-*n*-heptyloxycarbonylphenyliminomethyl)benzoate], 5.A.2

Yield 70%, m. p. 120.0˚C. ν_{max}: 2954, 2923, 2854, 2237, 1735, 1714, 1598, 1568, 1467, 1234, 1166, 1094, 1012 cm^{-1}; δ_H: 8.55 (s, 2H, 2 × -CH═N-), 8.38 (d, ^3J 8.32 Hz, 4H, Ar-H), 8.11 (d, ^3J 8.4 Hz, 4H, Ar-H), 8.09 (d, ^3J 8.32 Hz, 4H, Ar-H), 7.77 (t, ^3J 8.4 Hz, 1H, Ar-H), 7.49 (d, ^3J 8.4 Hz, 2H, Ar-H), 7.26 (d, ^3J 8.4 Hz, 4H, Ar-H), 4.33 (t, ^3J 6.64 Hz, 4H, 2× Ar-COO-CH_2-), 1.82-1.75 (quin, ^3J 6.68 Hz, 4H, 2 × Ar-COO-CH_2-$\underline{CH_2}$-), 1.46-1.28 (m, 16H, 2 × $(-CH_2-)_4$), 0.88 (t, ^3J 6.48 Hz, 6H, 2 × -CH_3); $C_{51}H_{51}N_3O_8$ requires C 73.45, H 6.16, N 5.04; found C 73.64, H 6.27, N 4.72 %.

2-Cyano-1, 3-phenylene bis [4-(4-*n*-octyloxycarbonylphenyliminomethyl)benzoate], 5.A.3

Yield 68%, m. p. 113.0˚C. ν_{max}: 2922, 2852, 2667, 1745, 1739, 1737, 1712, 1461, 1377, 1280 cm^{-1}; δ_H: 8.55 (s, 2H, 2 × -CH═N-), 8.38 (d, ^3J 8.32 Hz, 4H, Ar-H), 8.11 (d, ^3J 8.4 Hz, 4H, Ar-H), 8.09 (d, ^3J 8.32 Hz, 4H, Ar-H), 7.77 (t, ^3J 8.4 Hz, 1H, Ar-H), 7.49 (d, ^3J 8.4 Hz, 2H, Ar-H), 7.26

(d, ^{3}J 8.4 Hz, 4H, Ar-H), 4.33 (t, ^{3}J 6.64 Hz, 4H, 2× Ar-COO-CH_2-), 1.82-1.75 (quin, ^{3}J 6.68 Hz, 4H, 2 × Ar-COO-CH_2-$\underline{CH_2}$-), 1.46-1.28 (m, 20H, 2 × $(-CH_2-)_5$), 0.88 (t, ^{3}J 6.48 Hz, 6H, 2 × -CH_3); $C_{53}H_{55}N_3O_8$ requires C 73.85, H 6.43, N 4.87; found C 73.62, H 6.5, N 4.93 %.

2-Cyano-1, 3-phenylene bis [4-(4-*n*-nonyloxycarbonylphenyliminomethyl)benzoate], 5.A.4
Yield 72%, m. p. 115.5˚C. ν_{max}: 2922, 2852, 2667, 1748, 1736, 1734, 1716, 1461, 1377, 1280 cm^{-1}; δ_H: 8.55 (s, 2H, 2 × -CH=N-), 8.38 (d, ^{3}J 8.32 Hz, 4H, Ar-H), 8.11 (d, ^{3}J 8.4 Hz, 4H, Ar-H), 8.09 (d, ^{3}J 8.32 Hz, 4H, Ar-H), 7.77 (t, ^{3}J 8.4 Hz, 1H, Ar-H), 7.49 (d, ^{3}J 8.4 Hz, 2H, Ar-H), 7.26 (d, ^{3}J 8.4 Hz, 4H, Ar-H), 4.33 (t, ^{3}J 6.64 Hz, 4H, 2× Ar-COO-CH_2-), 1.82-1.75 (quin, ^{3}J 6.68 Hz, 4H, 2 × Ar-COO-CH_2-$\underline{CH_2}$-), 1.46-1.28 (m, 24H, 2 × $(-CH_2-)_6$), 0.88 (t, ^{3}J 6.48 Hz, 6H, 2 × -CH_3); $C_{55}H_{59}N_3O_8$ requires C 74.22, H 6.68, N 4.72; found C 74.60, H 6.74, N 4.72 %.

2-Cyano-1, 3-phenylene bis [4-(4-*n*-decyloxycarbonylphenyliminomethyl)benzoate], 5.A.5
Yield 75%, m. p. 118.0˚C. ν_{max}: 2922, 2852, 2237, 1755, 1730, 1728, 1714, 1598, 1463, 1377, 1271, 1242, 1107 cm^{-1}; δ_H: 8.55 (s, 2H, 2 × -CH=N-), 8.38 (d, ^{3}J 8.32 Hz, 4H, Ar-H), 8.11 (d, ^{3}J 8.4 Hz, 4H, Ar-H), 8.09 (d, ^{3}J 8.32 Hz, 4H, Ar-H), 7.77 (t, ^{3}J 8.4 Hz, 1H, Ar-H), 7.49 (d, ^{3}J 8.4 Hz, 2H, Ar-H), 7.26 (d, ^{3}J 8.4 Hz, 4H, Ar-H), 4.33 (t, ^{3}J 6.64 Hz, 4H, 2× Ar-COO-CH_2-), 1.82-1.75 (quin, ^{3}J 6.68 Hz, 4H, 2 × Ar-COO-CH_2-$\underline{CH_2}$-), 1.46-1.28 (m, 28H, 2 × $(-CH_2-)_7$), 0.88 (t, ^{3}J 6.48 Hz, 6H, 2 × -CH_3); $C_{57}H_{63}N_3O_8$ requires C 73.37, H 6.91, N 4.57; found C 73.0, H 6.68, N 4.29 %.

2-Cyano-1, 3-phenylene bis [4-(4-*n*-undecyloxycarbonylphenyliminomethyl)benzoate], 5.A.6
Yield 70%, m. p. 117.5˚C. ν_{max}: 2922, 2852, 2237, 1753, 1747, 1737, 1730, 1627, 1598, 1568, 1469, 1413, 1261, 1234, 1166, 1099, 1012 cm^{-1}; δ_H: 8.55 (s, 2H, 2 × -CH=N-), 8.38 (d, ^{3}J 8.32 Hz, 4H, Ar-H), 8.11 (d, ^{3}J 8.4 Hz, 4H, Ar-H), 8.09 (d, ^{3}J 8.32 Hz, 4H, Ar-H), 7.77 (t, ^{3}J 8.4 Hz, 1H, Ar-H), 7.49 (d, ^{3}J 8.4 Hz, 2H, Ar-H), 7.26 (d, ^{3}J 8.4 Hz, 4H, Ar-H), 4.33 (t, ^{3}J 6.64 Hz, 4H, 2× Ar-COO-CH_2-), 1.82-1.75 (quin, ^{3}J 6.68 Hz, 4H, 2 × Ar-COO-CH_2-$\underline{CH_2}$-), 1.46-1.28 (m, 32H, 2 × $(-CH_2-)_8$), 0.88 (t, ^{3}J 6.48 Hz, 6H, 2 × -CH_3); $C_{59}H_{67}N_3O_8$ requires C 74.81, H 7.14, N 4.44; found C 74.75, H 7.05, N 4.35 %.

2-Cyano-1, 3-phenylene bis [4-(4-*n*-dodecyloxycarbonylphenyliminomethyl) benzoate], 5.A.7

Yield 75%, m. p. 131.5˚C. ν_{max}: 2921, 2852, 1745, 1739, 1737, 1712, 1461, 1377, 1280 cm^{-1}; δ_H: 8.55 (s, 2H, 2 × -CH=N-), 8.38 (d, ^3J 8.32 Hz, 4H, Ar-H), 8.11 (d, ^3J 8.4 Hz, 4H, Ar-H), 8.09 (d, ^3J 8.32 Hz, 4H, Ar-H), 7.77 (t, ^3J 8.4 Hz, 1H, Ar-H), 7.49 (d, ^3J 8.4 Hz, 2H, Ar-H), 7.26 (d, ^3J 8.4 Hz, 4H, Ar-H), 4.33 (t, ^3J 6.64 Hz, 4H, 2× Ar-COO-CH_2-), 1.82-1.75 (quin, ^3J 6.68 Hz, 4H, 2 × Ar-COO-CH_2-$\underline{CH_2}$-), 1.46-1.28 (m, 36H, 2 × $(-CH_2-)_9$), 0.88 (t, ^3J 6.48 Hz, 6H, 2 × $-CH_3$); $C_{61}H_{71}N_3O_8$ requires C 75.2, H 7.35, N 4.31; found C 75.15, H 7.45, N 3.96 %.

2-Cyano-1, 3-phenylene bis [4-(4-*n*-tetradecyloxycarbonylphenyliminomethyl)benzoate], 5.A.8

Yield 78%, m. p. 125.5˚C. ν_{max}: 2954, 2918, 2850, 2239, 1741, 1710, 1625, 1596, 1473, 1282, 1261, 1242, 1089 cm^{-1}; δ_H: 8.55 (s, 2H, 2 × -CH=N-), 8.38 (d, ^3J 8.32 Hz, 4H, Ar-H), 8.11 (d, ^3J 8.4 Hz, 4H, Ar-H), 8.09 (d, ^3J 8.32 Hz, 4H, Ar-H), 7.77 (t, ^3J 8.4 Hz, 1H, Ar-H), 7.49 (d, ^3J 8.4 Hz, 2H, Ar-H), 7.26 (d, ^3J 8.4 Hz, 4H, Ar-H), 4.33 (t, ^3J 6.64 Hz, 4H, 2× Ar-COO-CH_2-), 1.82-1.75 (quin, ^3J 6.68 Hz, 4H, 2 × Ar-COO-CH_2-$\underline{CH_2}$-), 1.46-1.28 (m, 44H, 2 × $(-CH_2-)_{11}$), 0.88 (t, ^3J 6.48 Hz, 6H, 2 × $-CH_3$); $C_{65}H_{79}N_3O_8$ requires C 75.77, H 7.72, N 4.07; found C 75.31, H 7.56, N 4.21 %.

2-Cyano-1, 3-phenylene bis [4-(4-*n*-hexadecyloxycarbonylphenyliminomethyl)benzoate], 5.A.9

Yield 73%, m. p. 108.0˚C. ν_{max}: 2954, 2918, 2850, 2239, 1743, 1712, 1710, 1625, 1596, 1473, 1286, 1276, 1259, 1242, 1089 cm^{-1}; δ_H: 8.55 (s, 2H, 2 × -CH=N-), 8.38 (d, ^3J 8.32 Hz, 4H, Ar-H), 8.11 (d, ^3J 8.4 Hz, 4H, Ar-H), 8.09 (d, ^3J 8.32 Hz, 4H, Ar-H), 7.77 (t, ^3J 8.4 Hz, 1H, Ar-H), 7.49 (d, ^3J 8.4 Hz, 2H, Ar-H), 7.26 (d, ^3J 8.4 Hz, 4H, Ar-H), 4.33 (t, ^3J 6.64 Hz, 4H, 2× Ar-COO-CH_2-), 1.82-1.75 (quin, ^3J 6.68 Hz, 4H, 2 × Ar-COO-CH_2-$\underline{CH_2}$-), 1.46-1.28 (m, 52H, 2 × $(-CH_2-)_{13}$), 0.88 (t, ^3J 6.48 Hz, 6H, 2 × $-CH_3$); $C_{69}H_{87}N_3O_8$ requires C 76.28, H 8.07, N 3.87; found C 76.50, H 7.81, N 3.55 %.

2-Cyano-1, 3-phenylene bis [4-(4-*n*-octadecyloxycarbonylphenyliminomethyl)benzoate], 5.A.10

Yield 72%, m. p. 107.0˚C. ν_{max}: 2922, 2852, 2667, 1744, 1739, 1736, 1710, 1461, 1377, 1280 cm^{-1}; δ_H: 8.55 (s, 2H, 2 × -CH═N-), 8.38 (d, ^3J 8.32 Hz, 4H, Ar-H), 8.11 (d, ^3J 8.4 Hz, 4H, Ar-H), 8.09 (d, ^3J 8.32 Hz, 4H, Ar-H), 7.77 (t, ^3J 8.4 Hz, 1H, Ar-H), 7.49 (d, ^3J 8.4 Hz, 2H, Ar-H), 7.26 (d, ^3J 8.4 Hz, 4H, Ar-H), 4.33 (t, ^3J 6.64 Hz, 4H, 2× Ar-COO-CH$_2$-), 1.82-1.75 (quin, ^3J 6.68 Hz, 4H, 2 × Ar-COO-CH$_2$-$\underline{\mathrm{CH}_2}$-), 1.46-1.28 (m, 60H, 2 × (-CH$_2$-)$_{15}$), 0.88 (t, ^3J 6.48 Hz, 6H, 2 × -CH$_3$); $C_{71}H_{95}N_3O_8$ requires C 76.74, H 8.38, N 3.68; found C 76.70, H 8.28, N 3.53 %.

2-Nitro-1, 3-phenylene bis [4-(4-*n*-octyloxycarbonylphenyliminomethyl)benzoate], 5.B.1

Yield 75%, m. p. 85.5˚C. ν_{max}: 2922, 2852, 1745, 1742, 1738, 1712, 1461, 1377, 1280 cm^{-1}; δ_H: 8.53 (s, 2H, 2 × -CH═N-), 8.27 (d, ^3J 8.40 Hz, 4H, Ar-H), 8.10 (d, ^3J 8.52 Hz, 4H, Ar-H), 8.07 (d, ^3J 8.4 Hz, 4H, Ar-H), 7.69 (t, ^3J 8.52 Hz, 1H, Ar-H), 7.45 (d, ^3J 8.5 Hz, 2H, Ar-H), 7.25 (d, ^3J 8.52 Hz, 4H, Ar-H), 4.33 (t, ^3J 6.64 Hz, 4H, 2 × Ar-COO-CH$_2$-), 1.82-1.75 (quin, ^3J 6.76 Hz, 4H, 2 × Ar-COO-CH$_2$-$\underline{\mathrm{CH}_2}$-), 1.45-1.26 (m, 20H, 2 × (-CH$_2$-)$_5$), 0.88 (t, ^3J 6.48 Hz, 6H, 2 × -CH$_3$); $C_{52}H_{55}N_3O_{10}$ requires C 70.82, H 6.28, N 4.76; found C 70.43, H 6.49, N 4.66 %.

2-Nitro-1, 3-phenylene bis [4-(4-*n*-nonyloxycarbonylphenyliminomethyl)benzoate], 5.B.2

Yield 76%, m. p. 93.5˚C. ν_{max}: 2922, 2852, 1747, 1741, 1738, 1718, 1463, 1377, 1234 cm^{-1}; δ_H: 8.53 (s, 2H, 2 × -CH═N-), 8.27 (d, ^3J 8.40 Hz, 4H, Ar-H), 8.10 (d, ^3J 8.52 Hz, 4H, Ar-H), 8.07 (d, ^3J 8.4 Hz, 4H, Ar-H), 7.69 (t, ^3J 8.52 Hz, 1H, Ar-H), 7.45 (d, ^3J 8.5 Hz, 2H, Ar-H), 7.25 (d, ^3J 8.52 Hz, 4H, Ar-H), 4.33 (t, ^3J 6.64 Hz, 4H, 2 × Ar-COO-CH$_2$-), 1.82-1.75 (quin, ^3J 6.76 Hz, 4H, 2 × Ar-COO-CH$_2$-$\underline{\mathrm{CH}_2}$-), 1.45-1.26 (m, 24H, 2 × (-CH$_2$-)$_6$), 0.88 (t, ^3J 6.48 Hz, 6H, 2 × -CH$_3$); $C_{54}H_{59}N_3O_{10}$ requires C 71.22, H 6.53, N 4.61; found C 71.17, H 6.54, N 4.93 %.

2-Nitro-1, 3-phenylene bis [4-(4-*n*-decyloxycarbonylphenyliminomethyl)benzoate], 5.B.3

Yield 72%, m. p. 90.0˚C. ν_{max}: 2923, 2854, 1747, 1741, 1739, 1718, 1716, 1598, 1537, 1465, 1365, 1375, 1263 cm^{-1}; δ_H: 8.53 (s, 2H, 2×-CH═N-), 8.27 (d, ^3J 8.40 Hz, 4H, Ar-H), 8.10 (d, ^3J 8.52 Hz, 4H, Ar-H), 8.07 (d, ^3J 8.4 Hz, 4H, Ar-H), 7.69 (t, ^3J 8.52 Hz, 1H, Ar-H), 7.45 (d, ^3J 8.5 Hz, 2H, Ar-H), 7.25 (d, ^3J 8.52 Hz, 4H, Ar-H), 4.33 (t, ^3J 6.64 Hz, 4H, 2 × Ar-COO-CH$_2$-), 1.82-

1.75 (quin, ^3J 6.76 Hz, 4H, 2 × Ar-COO-CH$_2$-$\underline{CH_2}$-), 1.45-1.26 (m, 28H, 2 ×(-CH$_2$-)$_7$), 0.88 (t, ^3J 6.48 Hz, 6H, 2 × -CH$_3$); $C_{56}H_{63}N_3O_{10}$ requires C 71.70, H 6.76, N 4.47; found C 71.51, H 6.84, N 4.90 %.

2-Nitro-1, 3-phenylene bis [4-(4-*n*-undecyloxycarbonylphenyliminomethyl)benzoate], 5.B.4
Yield 70%, m. p. 89.0˚C. ν_{max}: 2922, 2852, 1741, 1718, 1708, 1463, 1377, 1265 cm^{-1}; δ_H: 8.53 (s, 2H, 2 × -CH═N-), 8.27 (d, ^3J 8.40 Hz, 4H, Ar-H), 8.10 (d, ^3J 8.52 Hz, 4H, Ar-H), 8.07 (d, ^3J 8.4 Hz, 4H, Ar-H), 7.69 (t, ^3J 8.52 Hz, 1H, Ar-H), 7.45 (d, ^3J 8.5 Hz, 2H, Ar-H), 7.25 (d, ^3J 8.52 Hz, 4H, Ar-H), 4.33 (t, ^3J 6.64 Hz, 4H, 2 × Ar-COO-CH$_2$-), 1.82-1.75 (quin, ^3J 6.76 Hz, 4H, 2 × Ar-COO-CH$_2$-$\underline{CH_2}$-), 1.45-1.26 (m, 32H, 2 × (-CH$_2$-)$_8$), 0.88 (t, ^3J 6.48 Hz, 6H, 2 × -CH$_3$); $C_{58}H_{67}N_3O_{10}$ requires C 72.10, H 6.98, N 4.76; found C 72.09, H 7.07, N 4.77 %.

2-Nitro-1, 3-phenylene bis [4-(4-*n*-dodecyloxycarbonylphenyliminomethyl)benzoate], 5.B.5
Yield 68%, m. p. 87.5˚C. ν_{max}: 2923, 1741, 1730, 1716, 1701, 1596, 1153, 1465, 1377, 1263, 1240 cm^{-1}; δ_H: 8.53 (s, 2H, 2 × -CH═N-), 8.27 (d, ^3J 8.40 Hz, 4H, Ar-H), 8.10 (d, ^3J 8.52 Hz, 4H, Ar-H), 8.07 (d, ^3J 8.4 Hz, 4H, Ar-H), 7.69 (t, ^3J 8.52 Hz, 1H, Ar-H), 7.45 (d, ^3J 8.5 Hz, 2H, Ar-H), 7.25 (d, ^3J 8.52 Hz, 4H, Ar-H), 4.33 (t, ^3J 6.64 Hz, 4H, 2 × Ar-COO-CH$_2$-), 1.82-1.75 (quin, ^3J 6.76 Hz, 4H, 2 × Ar-COO-CH$_2$-$\underline{CH_2}$-), 1.45-1.26 (m, 36H, 2 × (-CH$_2$-)$_9$), 0.88 (t, ^3J 6.48 Hz, 6H, 2 × -CH$_3$); $C_{60}H_{71}N_3O_{10}$ requires C 72.49, H 7.19, N 4.22; found C 72.48, H 7.27, N 4.68 %.

2-Nitro-1, 3-phenylene bis [4-(4-*n*-tetradecyloxycarbonylphenyliminomethyl)benzoate], 5.B.6
Yield 71%, m. p. 83.0˚C. ν_{max}: 2852, 2667, 1745, 1739, 1737, 1712, 1461, 1377, 1280 cm^{-1}; δ_H: 8.53 (s, 2H, 2 × -CH═N-), 8.27 (d, ^3J 8.40 Hz, 4H, Ar-H), 8.10 (d, ^3J 8.52 Hz, 4H, Ar-H), 8.07 (d, ^3J 8.4 Hz, 4H, Ar-H), 7.69 (t, ^3J 8.52 Hz, 1H, Ar-H), 7.45 (d, ^3J 8.5 Hz, 2H, Ar-H), 7.25 (d, ^3J 8.52 Hz, 4H, Ar-H), 4.33 (t, ^3J 6.64 Hz, 4H, 2 × Ar-COO-CH$_2$-), 1.82-1.75 (quin, ^3J 6.76 Hz, 4H, 2 × Ar-COO-CH$_2$-$\underline{CH_2}$-), 1.45-1.26 (m, 44H, 2 × (-CH$_2$-)$_{11}$), 0.88 (t, ^3J 6.48 Hz, 6H, 2 × -CH$_3$); $C_{64}H_{79}N_3O_{10}$ requires C 73.19, H 7.58, N 4.0; found C 73.12, H 7.42, N 4.04 %.

2-Nitro-1, 3-phenylene bis [4-(4-*n*-hexadecyloxycarbonylphenyliminomethyl)benzoate], 5.B.7

Yield 74%, m. p. 98.0˚C. ν_{max}: 2922, 2852, 1739, 1716, 1714, 1596, 1537, 1463, 1244, 1265 cm^{-1}; δ_H: 8.53 (s, 2H, 2 × -CH═N-), 8.27 (d, ^3J 8.40 Hz, 4H, Ar-H), 8.10 (d, ^3J 8.52 Hz, 4H, Ar-H), 8.07 (d, ^3J 8.4 Hz, 4H, Ar-H), 7.69 (t, ^3J 8.52 Hz, 1H, Ar-H), 7.45 (d, ^3J 8.5 Hz, 2H, Ar-H), 7.25 (d, ^3J 8.52 Hz, 4H, Ar-H), 4.33 (t, ^3J 6.64 Hz, 4H, 2 × Ar-COO-CH_2-), 1.82-1.75 (quin, ^3J 6.76 Hz, 4H, 2 × Ar-COO-CH_2-$\underline{CH_2}$-), 1.45-1.26 (m, 52H, 2 × $(-CH_2-)_{13}$), 0.88 (t, ^3J 6.48 Hz, 6H, 2 × -CH_3); $C_{68}H_{87}N_3O_{10}$ requires C 73.82, H 7.93, N 3.8; found C 73.69, H 7.96, N 4.23 %.

2-Nitro-1, 3-phenylene bis [4-(4-*n*-octadecyloxycarbonylphenyliminomethyl) benzoate], 5.B.8

Yield 76%, m. p. 81.5˚C. ν_{max}: 2920, 2848, 1749, 1732, 1712, 1606, 1537, 1467, 1363, 1242, 1166, 1101 cm^{-1}; δ_H: 8.53 (s, 2H, 2 × -CH═N-), 8.27 (d, ^3J 8.40 Hz, 4H, Ar-H), 8.10 (d, ^3J 8.52 Hz, 4H, Ar-H), 8.07 (d, ^3J 8.4 Hz, 4H, Ar-H), 7.69 (t, ^3J 8.52 Hz, 1H, Ar-H), 7.45 (d, ^3J 8.5 Hz, 2H, Ar-H), 7.25 (d, ^3J 8.52 Hz, 4H, Ar-H), 4.33 (t, ^3J 6.64 Hz, 4H, 2 × Ar-COO-CH_2-), 1.82-1.75 (quin, ^3J 6.76 Hz, 4H, 2 × Ar-COO-CH_2-$\underline{CH_2}$-), 1.45-1.26 (m, 60H, 2 × $(-CH_2-)_{15}$), 0.88 (t, ^3J 6.48 Hz, 6H, 2 × -CH_3); $C_{72}H_{95}N_3O_{10}$ requires C 74.39, H 8.24, N 3.61; found C 73.97, H 8.19, N 3.42 %.

2-Cyano-1, 3-phenylene bis [4-(4-*n*-decyloxycarbonylbenzylideneamino)benzoate], 5.C.1

4-(4-*n*-Decyloxycarbonylbenzylideneamino)benzoic acid, **5.e.1** (0.4g, 0.98 mmol) was reacted with 1,3-dihydroxybenzene, **5.iv** (0.066g, 0.49 mmol) in dry dichloromethane in presence of DCC (0.22g, 1.1 mmol) and a catalytic amount of DMAP. The mixture was stirred at room temperature for 24 hours. The precipitated *N*, *N'*-dicyclohexylurea was filtered off and the solvent from the filtrate was evaporated. The residue was dissolved in chloroform and filtered through a column of basic alumina. The product thus obtained on removal of the solvent was further purified by repeated crystallization using a mixture of chloroform and acetonitrile. Yield: 0.35g (79%), m. p. 123.5˚C. ν_{max}: 2922, 2852, 2235, 1749, 1735, 1718, 1716, 1595, 1569, 1467, 1413, 1274, 1259, 1234, 1164 cm^{-1}; δ_H: 8.51 (s, 2H, 2 × -CH═N-), 8.30 (d, ^3J 8.52 Hz, 4H, Ar-H), 8.17 (d, ^3J 8.28 Hz, 4H, Ar-H), 8.01 (d, ^3J 8.32 Hz, 4H, Ar-H), 7.74 (t, ^3J 8.44 Hz, 1H, Ar-H), 7.46 (d, ^3J 8.4 Hz, 2H, Ar-H), 7.32 (d, ^3J 8.52 Hz, 4H, Ar-H), 4.35 (t, ^3J 6.64 Hz, 4H, 2 × Ar-COO-CH_2-), 1.83-1.76

(quin, ^{3}J 6.72 Hz, 4H, 2 × Ar-COO-CH_2-$\underline{CH_2}$-), 1.46-1.26 (m, 28H, 2 × (-CH_2-)$_7$), 0.87 (t, ^{3}J 6.56 Hz, 6H, 2 × -CH_3); $C_{57}H_{63}N_3O_8$ requires C 74.37, H 6.91, N 4.57; found C 74.17, H 6.85, N 4.74 %.

2-Cyano-1, 3-phenylene bis [4-(4-*n*-undecyloxycarbonylbenzylideneamino)benzoate], 5.C.2

Yield 78%, m. p. 128.5°C. ν_{max}: 2922, 2852, 2235, 1749, 1735, 1718, 1716, 1595, 1569, 1467, 1413, 1274, 1259, 1234, 1164 cm^{-1}; δ_H: 8.51 (s, 2H, 2 × -CH═N-), 8.30 (d, ^{3}J 8.52 Hz, 4H, Ar-H), 8.17 (d, ^{3}J 8.28 Hz, 4H, Ar-H), 8.01 (d, ^{3}J 8.32 Hz, 4H, Ar-H), 7.74 (t, ^{3}J 8.44 Hz, 1H, Ar-H), 7.46 (d, ^{3}J 8.4 Hz, 2H, Ar-H), 7.32 (d, ^{3}J 8.52 Hz, 4H, Ar-H), 4.35 (t, ^{3}J 6.64 Hz, 4H, 2 × Ar-COO-CH_2-), 1.83-1.76 (quin, ^{3}J 6.72 Hz, 4H, 2 × Ar-COO-CH_2-$\underline{CH_2}$-), 1.46-1.26 (m, 32H, 2 × (-CH_2-)$_8$), 0.87 (t, ^{3}J 6.56 Hz, 6H, 2 × -CH_3); $C_{59}H_{67}N_3O_8$ requires C 74.81, H 7.14, N 4.44; found C 74.70, H 6.99, N 4.38 %.

2-Cyano-1, 3-phenylene bis [4-(4-*n*-dodecyloxycarbonylbenzylideneamino)benzoate], 5.C.3

Yield 80%, m. p. 114.0°C. ν_{max}: 2922, 2852, 2235, 1749, 1735, 1718, 1716, 1595, 1569, 1467, 1413, 1274, 1259, 1234, 1164 cm^{-1}; δ_H: 8.51 (s, 2H, 2 × -CH═N), 8.30 (d, ^{3}J 8.52 Hz, 4H, Ar-H), 8.17 (d, ^{3}J 8.28 Hz, 4H, Ar-H), 8.01 (d, ^{3}J 8.32 Hz, 4H, Ar-H), 7.74 (t, ^{3}J 8.44 Hz, 1H, Ar-H), 7.46 (d, ^{3}J 8.4 Hz, 2H, Ar-H), 7.32 (d, ^{3}J 8.52 Hz, 4H, Ar-H), 4.35 (t, ^{3}J 6.64 Hz, 4H, 2 × Ar-COO-CH_2-), 1.83-1.76 (quin, ^{3}J 6.72 Hz, 4H, 2 × Ar-COO-CH_2-$\underline{CH_2}$-), 1.46-1.26 (m, 36H, 2 × (-CH_2-)$_9$), 0.87 (t, ^{3}J 6.56 Hz, 6H, 2 × -CH_3); $C_{61}H_{71}N_3O_8$ requires C 75.21, H 7.35, N 4.31; found C 75.21, H 7.31, N 4.73 %.

2-Cyano-1, 3-phenylene bis [4-(4-*n*-tetradecyloxycarbonylbenzylideneamino)benzoate], 5.C.4

Yield 76%, m. p. 96.5°C. ν_{max}: 2954, 2918, 2850, 2241, 1737, 1714, 1625, 1593, 1571, 1469, 1413, 1361, 1261, 1166, 1120 cm^{-1}; δ_H: 8.51 (s, 2H, 2 × -CH═N), 8.30 (d, ^{3}J 8.52 Hz, 4H, Ar-H), 8.17 (d, ^{3}J 8.28 Hz, 4H, Ar-H), 8.01 (d, ^{3}J 8.32 Hz, 4H, Ar-H), 7.74 (t, ^{3}J 8.44 Hz, 1H, Ar-H), 7.46 (d, ^{3}J 8.4 Hz, 2H, Ar-H), 7.32 (d, ^{3}J 8.52 Hz, 4H, Ar-H), 4.35 (t, ^{3}J 6.64 Hz, 4H, 2 × Ar-COO-CH_2-), 1.83-1.76 (quin, ^{3}J 6.72 Hz, 4H, 2 × Ar-COO-CH_2-$\underline{CH_2}$-), 1.46-1.26 (m, 44H, 2 × (-CH_2-)$_{11}$), 0.87 (t, ^{3}J 6.56 Hz, 6H, 2 × -CH_3); $C_{65}H_{79}N_3O_8$ requires C 75.77, H 7.72, N 4.07; found C 75.77, H 7.56, N 4.26 %.

2-Cyano-1, 3-phenylene bis [4-(4-*n*-hexadecyloxycarbonylbenzylideneamino)benzoate], 5.C.5

Yield 79%, m. p. 103.0°C. ν_{max}: 2954, 2918, 2850, 2241, 1739, 1733, 1712, 1625, 1593, 1571, 1469, 1413, 1361, 1261, 1166, 1120 cm^{-1}; δ_H: 8.51 (s, 2H, 2 × -CH═N-), 8.30 (d, ^3J 8.52 Hz, 4H, Ar-H), 8.17 (d, ^3J 8.28 Hz, 4H, Ar-H), 8.01 (d, ^3J 8.32 Hz, 4H, Ar-H), 7.74 (t, ^3J 8.44 Hz, 1H, Ar-H), 7.46 (d, ^3J 8.4 Hz, 2H, Ar-H), 7.32 (d, ^3J 8.52 Hz, 4H, Ar-H), 4.35 (t, ^3J 6.64 Hz, 4H, 2 × Ar-COO-CH_2-), 1.83-1.76 (quin, ^3J 6.72 Hz, 4H, 2 × Ar-COO-CH_2-$\underline{CH_2}$-), 1.46-1.26 (m, 52H, 2 × (-CH_2-)$_{13}$), 0.87 (t, ^3J 6.56 Hz, 6H, 2 × -CH_3); $C_{69}H_{87}N_3O_8$ requires C 76.28, H 8.07, N 3.87; found C 76.0, H 7.96, N 3.67 %.

2-Cyano-1, 3-phenylene bis [4-(4-*n*-octadecyloxycarbonylbenzylideneamino)benzoate], 5.C.6

Yield 81%, m. p. 107.5°C. ν_{max}: 2952, 2918, 2850, 2241, 1741, 1712, 1710, 1625, 1596, 1473, 1280, 1261, 1244, 1089 cm^{-1}; δ_H: 8.51 (s, 2H, 2 × -CH═N-), 8.30 (d, ^3J 8.52 Hz, 4H, Ar-H), 8.17 (d, ^3J 8.28 Hz, 4H, Ar-H), 8.01 (d, ^3J 8.32 Hz, 4H, Ar-H), 7.74 (t, ^3J 8.44 Hz, 1H, Ar-H), 7.46 (d, ^3J 8.4 Hz, 2H, Ar-H), 7.32 (d, ^3J 8.52 Hz, 4H, Ar-H), 4.35 (t, ^3J 6.64 Hz, 4H, 2 × Ar-COO-CH_2-), 1.83-1.76 (quin, ^3J 6.72 Hz, 4H, 2 × Ar-COO-CH_2-$\underline{CH_2}$-), 1.46-1.26 (m, 60H, 2 × (-CH_2-)$_{15}$), 0.87 (t, ^3J 6.56 Hz, 6H, 2 × -CH_3); $C_{74}H_{95}N_3O_8$ requires C 76.74, H 8.38, N 3.68; found C 76.34, H 8.44, N 3.53 %.

2-Nitro-1, 3-phenylene bis [4-(4-*n*-decyloxycarbonylbenzylideneamino)benzoate], 5.D.1

Yield 78%, m. p. 106.5°C. ν_{max}: 2922, 2852, 1747, 1732, 1631, 1595, 1535, 1467, 1363, 1226, 1164 cm^{-1}; δ_H: 8.50 (s, 2H, 2 × -CH═N-), 8.20 (d, ^3J 8.52 Hz, 4H, Ar-H), 8.17 (d, ^3J 8.28 Hz, 4H, Ar-H), 8.01 (d, ^3J 8.32 Hz, 4H, Ar-H), 7.67 (t, ^3J 8.44 Hz, 1H, Ar-H), 7.42 (d, ^3J 8.4 Hz, 2H, Ar-H), 7.29 (d, ^3J 8.52 Hz, 4H, Ar-H), 4.35 (t, ^3J 6.64 Hz, 4H, 2 × Ar-COO-CH_2-), 1.83-1.76 (quin, ^3J 6.68 Hz, 4H, 2 × Ar-COO-CH_2-$\underline{CH_2}$-), 1.46-1.26 (m, 28H, 2 × (-CH_2-)$_7$), 0.87 (t, ^3J 6.44 Hz, 6H, 2 × -CH_3); $C_{56}H_{63}N_3O_{10}$ requires C 71.69, H 6.77, N 4.48; found C 71.26, H 6.78, N 4.21 %.

2-Nitro-1, 3-phenylene bis [4-(4-*n*-undecyloxycarbonylbenzylideneamino)benzoate], 5.D.2

Yield 80%, m. p. 101.0˚C. ν_{max}: 2922, 2852, 1747, 1732, 1631, 1595, 1535, 1467, 1363, 1226, 1164 cm^{-1}; δ_H: 8.50 (s, 2H, 2 × -CH═N-), 8.20 (d, ^3J 8.52 Hz, 4H, Ar-H), 8.17 (d, ^3J 8.28 Hz, 4H, Ar-H), 8.01 (d, ^3J 8.32 Hz, 4H, Ar-H), 7.67 (t, ^3J 8.44 Hz, 1H, Ar-H), 7.42 (d, ^3J 8.4 Hz, 2H, Ar-H), 7.29 (d, ^3J 8.52 Hz, 4H, Ar-H), 4.35 (t, ^3J 6.64 Hz, 4H, 2 × Ar-COO-CH$_2$-), 1.83-1.76 (quin, ^3J 6.68 Hz, 4H, 2 × Ar-COO-CH$_2$-$\underline{\text{CH}}_2$-), 1.46-1.26 (m, 32H, 2 × (-CH$_2$-)$_8$), 0.87 (t, ^3J 6.44 Hz, 6H, 2 × -CH$_3$); $C_{58}H_{67}N_3O_{10}$ requires C 72.10, H 6.98, N 4.35; found C 71.67, H 7.19, N 4.27 %.

2-Nitro-1, 3-phenylene bis [4-(4-*n*-dodecyloxycarbonylbenzylideneamino)benzoate], 5.D.3

Yield 80%, m. p. 91.0˚C. ν_{max}: 2922, 2852, 1747, 1732, 1631, 1595, 1535, 1467, 1363, 1226, 1164 cm^{-1}; δ_H: 8.50 (s, 2H, 2 × -CH═N-), 8.20 (d, ^3J 8.52 Hz, 4H, Ar-H), 8.17 (d, ^3J 8.28 Hz, 4H, Ar-H), 8.01 (d, ^3J 8.32 Hz, 4H, Ar-H), 7.67 (t, ^3J 8.44 Hz, 1H, Ar-H), 7.42 (d, ^3J 8.4 Hz, 2H, Ar-H), 7.29 (d, ^3J 8.52 Hz, 4H, Ar-H), 4.35 (t, ^3J 6.64 Hz, 4H, 2 × Ar-COO-CH$_2$-), 1.83-1.76 (quin, ^3J 6.68 Hz, 4H, 2 × Ar-COO-CH$_2$-$\underline{\text{CH}}_2$-), 1.46-1.26 (m, 36H, 2 × (-CH$_2$-)$_9$), 0.87 (t, ^3J 6.44 Hz, 6H, 2 × -CH$_3$); $C_{60}H_{71}N_3O_{10}$ requires C 72.49, H 7.19, N 4.07; found C 72.17, H 7.19, N 4.22 %.

2-Nitro-1, 3-phenylene bis [4-(4-*n*-tetradecyloxycarbonylbenzylideneamino)benzoate], 5.D.4

Yield 82%, m. p. 93.0˚C. ν_{max}: 2954, 2918, 2848, 1741, 1732, 1724, 1710, 1595, 1537, 1469, 1363, 1338, 1267, 1091 cm^{-1}; δ_H: 8.50 (s, 2H, 2 × -CH═N-), 8.20 (d, ^3J 8.52 Hz, 4H, Ar-H), 8.17 (d, ^3J 8.28 Hz, 4H, Ar-H), 8.01 (d, ^3J 8.32 Hz, 4H, Ar-H), 7.67 (t, ^3J 8.44 Hz, 1H, Ar-H), 7.42 (d, ^3J 8.4 Hz, 2H, Ar-H), 7.29 (d, ^3J 8.52 Hz, 4H, Ar-H), 4.35 (t, ^3J 6.64 Hz, 4H, 2 × Ar-COO-CH$_2$-), 1.83-1.76 (quin, ^3J 6.68 Hz, 4H, 2 × Ar-COO-CH$_2$-$\underline{\text{CH}}_2$-), 1.46-1.26 (m, 44H, 2 × (-CH$_2$-)$_{11}$), 0.87 (t, ^3J 6.44 Hz, 6H, 2 × -CH$_3$); $C_{64}H_{79}N_3O_{10}$ requires C 73.19, H 7.58, N 4.07; found C 72.85, H 7.36, N 3.88 %.

2-Nitro-1, 3-phenylene bis [4-(4-*n*-hexadecyloxycarbonylbenzylideneamino)benzoate], 5.D.5

Yield 79%, m. p. 89.5˚C. ν_{max}: 2954, 2920, 2848, 1749, 1732, 1730, 1726, 1595, 1537, 1469, 1363, 1269, 1242, 1166, 1103 cm^{-1}; δ_H: 8.50 (s, 2H, 2 × -CH═N), 8.20 (d, ^3J 8.52 Hz, 4H, Ar-H), 8.17 (d, ^3J 8.28 Hz, 4H, Ar-H), 8.01 (d, ^3J 8.32 Hz, 4H, Ar-H), 7.67 (t, ^3J 8.44 Hz, 1H, Ar-H), 7.42 (d, ^3J 8.4 Hz, 2H, Ar-H), 7.29 (d, ^3J 8.52 Hz, 4H, Ar-H), 4.35 (t, ^3J 6.64 Hz, 4H, 2 × Ar-COO-CH_2-), 1.83-1.76 (quin, ^3J 6.68 Hz, 4H, 2 × Ar-COO-CH_2-$\underline{CH_2}$-), 1.46-1.26 (m, 52H, 2 × (-CH_2-)$_{13}$), 0.87 (t, ^3J 6.44 Hz, 6H, 2 × -CH_3); $C_{68}H_{87}N_3O_{10}$ requires C 73.82, H 7.93, N 3.8; found C 73.59, H 7.89, N 3.48 %.

2-Nitro-1, 3-phenylene bis [4-(4-*n*-octadecyloxycarbonylbenzylideneamino)benzoate], 5.D.6

Yield 82%, m. p. 92.0˚C. ν_{max}: 2954, 2918, 2848, 1741, 1730, 1724, 1710, 1595, 1541, 1469, 1269, 1242, 1166, 1103 cm^{-1}; δ_H: 8.50 (s, 2H, 2 × -CH═N-), 8.20 (d, ^3J 8.52 Hz, 4H, Ar-H), 8.17 (d, ^3J 8.28 Hz, 4H, Ar-H), 8.01 (d, ^3J 8.32 Hz, 4H, Ar-H), 7.67 (t, ^3J 8.44 Hz, 1H, Ar-H), 7.42 (d, ^3J 8.4 Hz, 2H, Ar-H), 7.29 (d, ^3J 8.52 Hz, 4H, Ar-H), 4.35 (t, ^3J 6.64 Hz, 4H, 2 × Ar-COO-CH_2-), 1.83-1.76 (quin, ^3J 6.68 Hz, 4H, 2 × Ar-COO-CH_2-$\underline{CH_2}$-), 1.46-1.26 (m, 60H, 2 × (-CH_2-)$_{15}$), 0.87 (t, ^3J 6.44 Hz, 6H, 2 × -CH_3); $C_{72}H_{95}N_3O_{10}$ requires C 74.39, H 8.24, N 3.61; found C 73.99, H 8.17, N 3.39 %.

References

[1] G. Pelzl, S. Diele, A. Jakli, C. Lischka, I. Wirth and W. Weissflog, *Liq. Cryst.*, **26**, 135 (1999).

[2] R. Amaranatha Reddy and B. K. Sadashiva, *Liq. Cryst.*, **29**, 1365 (2002).

[3] R. Amaranatha Reddy and B. K. Sadashiva, *Liq. Cryst.*, **30**, 273 (2003).

[4] H. N. Shreenivasa Murthy and B. K. Sadashiva, *Liq. Cryst.*, **30**, 1051 (2003).

[5] H. N. Shreenivasa Murthy and B. K. Sadashiva, *J. Mater. Chem.*, **13**, 2863 (2003).

[6] G. Pelzl, M. W. Schröder, U. Dunemann, S. Diele, W. Weissflog, C. Jones, D. Coleman, N. A. Clark, R. Stannarius, J. Li, B. Das, and S. Grande, *J. Mater. Chem.*, **14**, 2492 (2004).

[7] G. Heppke, D. D. Parghi and H. Sawade, *Ferroelectrics*, **243**, 269 (2000).

[8] G. Heppke, D. D. Parghi and H. Sawade, *Liq. Cryst.*, **27**, 313 (2000).

[9] D. M. Walba, E. Körblova, R. Shao, J. -E. Maclennan, D. R. Link, M. A. Glaser and N. A. Clark, *Science,* **288,** 2181(2000).

[10] C. K. Lee, A. Primak, A. Jakli, E. J. Cho, W. C. Zin and L. C. Chien, *Liq. Cryst.*, **28**, 1293 (2001).

[11] D. S. Shankar Rao, G. G. Nair, S. Krishna Prasad, S. Anita Nagamani and C. V. Yelamaggad, *Liq. Cryst.*, **28**, 1239 (2001).

[12] R. Amaranatha Reddy and C. Tschierske, *J. Mater. Chem.*, **16**, 907 (2006).

[13] D. A. Coleman, J. Fernsler, N. Chattham, M. Nakata, Y. Takanishi, E. Körblova, D. R. Link, R. -F. Shao, W. G. Jang, J. E. Maclennan, O. Mondainn-Monval, C. Boyer, W. Weissflog, G. Pelzl, L. -C. Chien, J. Zasadzinski, J. Watanabe, D. M. Walba, H. Takezoe and N. A. Clark, *Science*, **301**, 1204 (2003).

[14] C. L. Folcia, J. Extebarria, J. Ortega and M. B. Ros, *Phys. Rev. E,* **72**, 041709 (2005).

[15] C. A. Hunter and J. K. M. Sanders, *J. Am. Chem. Soc.*, **112**, 5525 (1990).

[16] S-W. Kang, R. Amaranatha Reddy, B. K. Sadashiva and S. Kumar, presented at the *International Liquid Crystal Conference*, Ljubljana, July 4-9, book of abstracts, SYN-P141 (2004).

[17] J. Thisayukta, Y. Nakayama and J. Watanabe, *Liq. Cryst.*, **27**, 1129 (2000).

[18] J. Thisayukta, Y. Nakayama, S. Kawauchi, H. Takezoe and J. Watanabe, *J. Am. Chem. Soc.*, **122**, 7441 (2000).

[19] H. N. Shreenivasa Murthy and B. K. Sadashiva, *Liq. Cryst.*, **29**, 1223 (2002).

[20] G. Dantlgraber, A. Eremin, S. Diele, A. Hauser, H. Kresse, G. Pelzl and C. Tschierske, *Angew. Chem. Int. Ed. Engl.*, **41**, 2408 (2002).

[21] G. Dantlgraber, S. Diele and C. Tschierske, *Chem. Commun*., 2768 (2002).

[22] A. Eremin, S. Diele, G. Pelzl and W. Weissflog, *Phys. Rev. E,* **67**, 020702 (2003).

[23] J. Ortega, C. L. Folcia, J. Etxebarria, N. Gimeno and M. B. Ros, *Phys. Rev. E.*, **68**, 011707 (2003).

[24] M. W. Schröder, S. Diele, G. Pelzl, U. Dunemann, H. Kresse and W. Weissflog, *J. Mater. Chem*., **13**, 1877 (2003). (b) M. W. Schröder, G. Pelzl, U. Dunemann, and W. Weissflog, *Liq. Cryst*., **31**, 633 (2004).

[25] R. Amaranatha Reddy and B. K. Sadashiva, *J. Mater. Chem*., **14**, 1936 (2004).

[26] C. Keith, R. Amaranatha Reddy, H. Hahn, H. Lang and C. Tschierske, *Chem. Commun.*, 1898 (2004).

[27] C. Keith, R. Amaranatha Reddy and C. Tschierske, *Chem. Commun.,* 871 (2005).

[28] H. N. Shreenivasa Murthy and B. K. Sadashiva, *Liq. Cryst*., **31**, 361 (2004).